Energy & Environmental Science

www.rsc.org/ees

Volume 1 | Number 1 | July 2008 | Pages 1–196

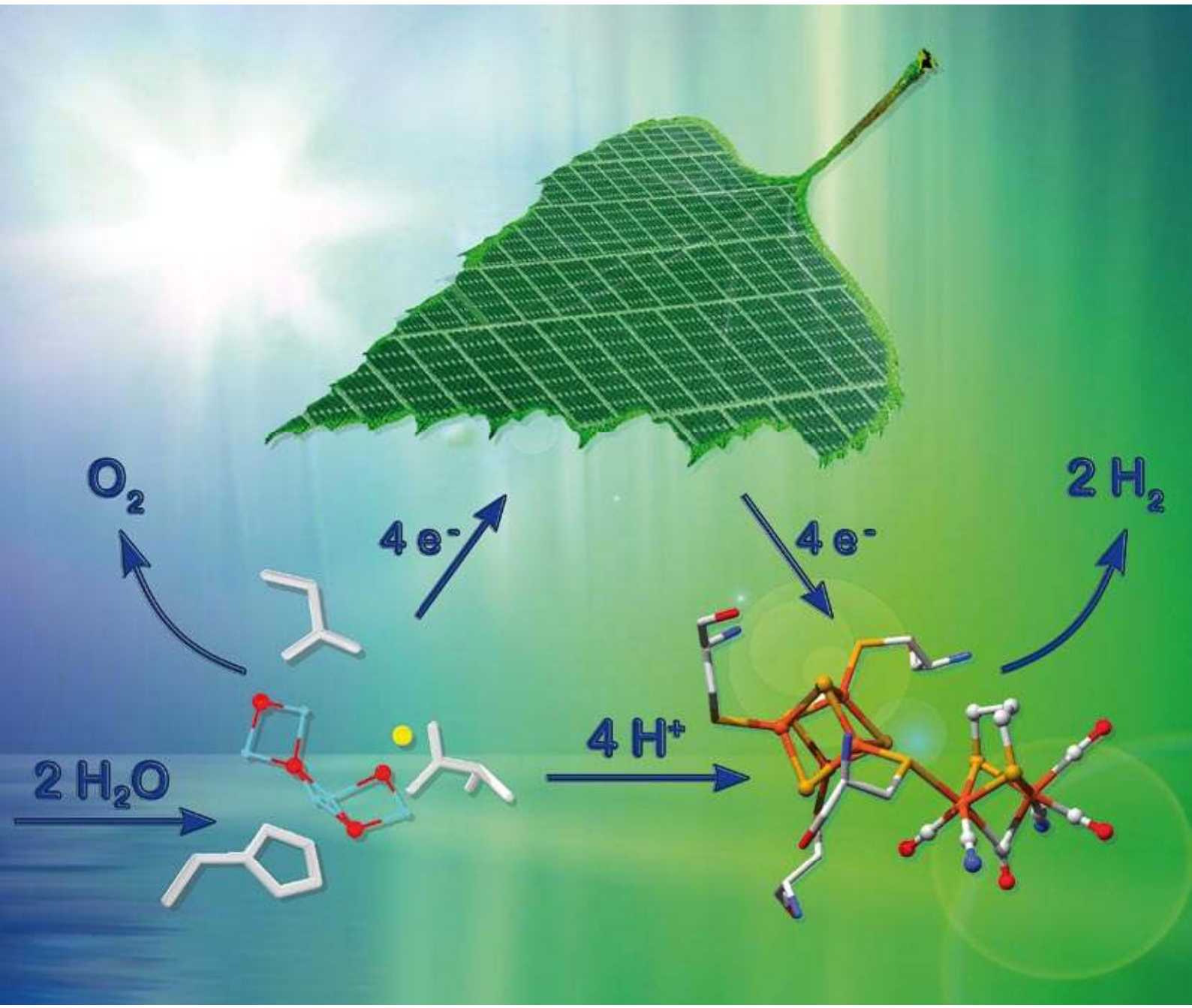

ISSN 1754-5692

COVER ARTICLE
Wolfgang Lubitz *et al.*
Solar water-splitting into H_2 and O_2: design principles of photosystem II and hydrogenases

REVIEW
Andrew Peterson *et al.*
Thermochemical biofuel production in hydrothermal media: a review of sub- and supercritical water technologies

RSC Publishing

1754-5692(2008)1:1;1-6

Solar water-splitting into H_2 and O_2: design principles of photosystem II and hydrogenases

Wolfgang Lubitz,* Edward J. Reijerse and Johannes Messinger†*

Received 27th May 2008, Accepted 17th June 2008
First published as an Advance Article on the web 30th June 2008
DOI: 10.1039/b808792j

This review aims at presenting the principles of water-oxidation in photosystem II and of hydrogen production by the two major classes of hydrogenases in order to facilitate application for the design of artificial catalysts for solar fuel production.

1. Introduction

Practically all life on earth depends directly or indirectly on photosynthesis. This therefore arguably most important chemical process on our planet[1–3] stores the sun's energy in chemical compounds (carbohydrates). The products of photosynthesis are the only renewable source of food. Photosynthesis also created our oxygen-rich atmosphere by water oxidation and thereby laid the basis for the formation of the protective ozone layer in the stratosphere. These events enabled the development of higher life on earth. Furthermore, all fossil fuels – oil, coal and natural gas – have been created from products of photosynthesis over the last 2.5 billion years. The rash and unsolicitous exploitation of these valuable resources during the past 1 to 2 centuries led to an enormous increase of energy usage in our society, which is still increasing in spite of the limited resources.[4] The burning of carbon-rich fuels also led to a significant rise of carbon dioxide (CO_2) levels in the atmosphere, a greenhouse gas that contributes to the global climate change with many adverse effects on our planet and human life.[5]

Max Planck Institut für Bioanorganische Chemie, Stiftstrasse 34-36, 45470 Mülheim, Ruhr, Germany. E-mail: lubitz@mpi-muelheim.mpg.de; Fax: +49 208 306 3955; Tel: +49 208 3063614
† New address: Department of Chemistry, Umeå University, S - 901 87 Umeå, Sweden, johannes.messinger@chem.umu.se.

The economical and socio-political consequences of the shortage of fossil fuels are already felt today. With the increase of world population and economic growth the global energy demand will continue to increase in the coming decades. Thus, it is high time to find alternative, sustainable energy resources. An obvious idea is to exploit the abundant energy of the sun: the energy hitting the surface of the earth by far exceeds human needs.[6] Solar energy has an enormous potential as clean, abundant and economical energy source, but must first be captured and converted into useful forms of energy. This includes conversion into heat, electricity and (chemical) fuels. In particular the efficient production of a clean, storable "solar fuel" would represent a very important breakthrough in scientific research.[7] Such a fuel must be formed from abundant, inexpensive materials such as water, which could be split into molecular oxygen and molecular hydrogen. Hydrogen is often considered to be the ideal fuel of the future since its combustion generates only water. The problems of H_2 generation, storage and transport have been intensively discussed in recent years.[8–11]

A promising way for light-driven water splitting would be to mimic the molecular and supramolecular organization of the natural photosynthetic system, *i.e.* "artificial photosynthesis".[12,13] However, many obstacles must be overcome. One of the major difficulties is the coupling of the light-induced (one-photon) one-electron charge separation to the multi-electron catalytic processes leading to water oxidation and fuel

W. Lubitz

E. Reijerse

J. Messinger

W. Lubitz is director of the MPI for Bioinorganic Chemistry and a specialist in advanced EPR techniques. He has a strong interest in both water-splitting and hydrogen production.

E. Reijerse is working on hydrogenases using FTIR and EPR/ENDOR spectroscopies.

J. Messinger is analyzing photosynthetic and artificial water-splitting employing O_2 measurements, mass spectrometry (MIMS), EPR and XAS.

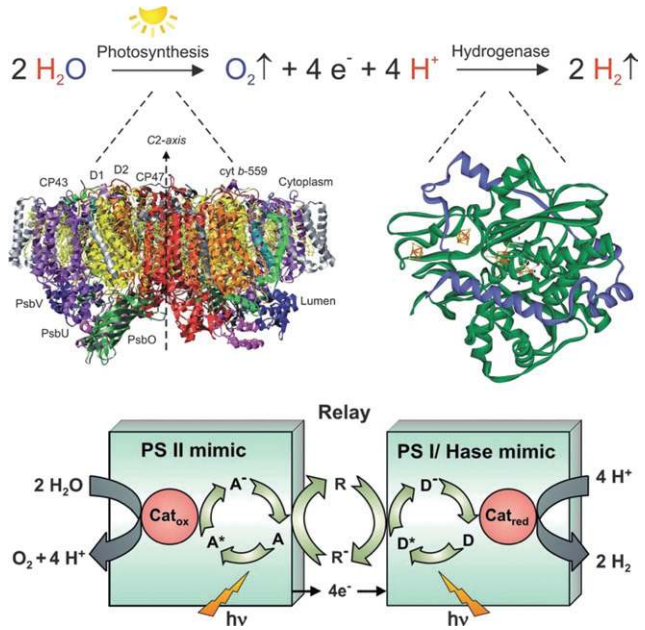

Fig. 1 Light induced water splitting by photosystem II in photosynthesis and hydrogen production by an [FeFe] hydrogenase shown together with the structure of respective protein complexes[17,18] and a possible scheme[19] for mimicking the natural process.

production. Another problem is the sensitivity and the limited lifetime of isolated native enzymes and current artificial devices.

Light-induced water-splitting and release of oxygen and protons is performed in nature in oxygenic photosynthesis by green plants, algae and cyanobacteria. The responsible highly complex enzyme is called photosystem (PS) II.[14] Many green algae and cyanobacteria also contain an enzyme that can convert the released protons into dihydrogen. This enzyme is called hydrogenase.[15,16] The process is depicted in Fig. 1, together with a view of the respective protein complexes[17,18] and a possible scheme mimicking the natural process *in vitro*.[19]

Photosystem II and several hydrogenases have been crystallized and structurally analyzed by X-ray crystallography[17,18] in recent years. The active sites contain complex multinuclear transition metal clusters that have been the subject of intense spectroscopic investigations aiming at a detailed understanding of their structure and function. Slowly a mechanistic understanding of these important processes is developing.

Knowledge of the basic principles of water oxidation and hydrogen conversion in nature is a goal of major importance both for basic research and possible application in our society. This would allow us to use the organisms – or the isolated enzymes – in biotechnological processes.[20–23] Furthermore, it would provide the foundation for designing biomimetic – or bioinspired – artificial catalysts for large-scale water splitting and hydrogen production in the future.

2. Water oxidation

Oxygenic photosynthesis was 'invented' on earth about 2.5 billion years ago at the level of cyanobacteria[24,25] and resulted in an enormous evolutionary advantage for these organisms since it allowed them to exploit the nearly unlimited electron source water. It is therefore surprising that evolution has, in contrast to for example hydrogenases (see below), created only one unique catalyst capable of performing light-induced water-splitting, which is known as photosystem II (PSII). It is also remarkable that so far only very minor differences have been found on the level of the water-splitting complex between different organisms such as higher plants, green algae and cyanobacteria. This uniqueness underpins the high level of complexity that is required to perform this strongly oxidizing reaction within a protein matrix. Although not all facets are yet known, several important features of the water-splitting reaction in PSII have been unraveled due to intense research efforts by many groups in the field (for recent reviews see[26–34]). These key features will be briefly outlined below, and their possible significance for constructing artificial catalysts for the water-splitting half-reaction (1) is discussed.

$$2H_2O \rightarrow O_2 + 4H^+ + 4e^- \quad (1)$$

2.1 Photosystem II

Photosystem II is an integral part of the thylakoid membrane. In the thermophilic cyanobacterium *Thermosynechococcus (T.) elongatus* it consist of about 20 protein subunits that harbor 77 cofactors: 35 Chl*a*; 14 lipids (+ 3 detergent molecules); 11 β-carotenes; 2 plastoquinones, PQ; 2 pheophytines, Pheo; 1 Mn_4O_xCa complex, 2 haem Fe; 1 non-haem Fe; 1 hydrogencarbonate, HCO_3^-.[18,35] In addition Cl^- is a known cofactor of water-splitting,[36,37] but was not yet identified in crystal structures. The overall reaction of PSII is that of a light-driven water: plastoquinone oxidoreductase:

$$2H_2O + 2PQ + 4H^+_{stroma} \xrightarrow{4h\nu} O_2 + 2PQH_2 + 4H^+_{lumen} \quad (2)$$

PSII utilizes visible light (~400–700 nm) to drive this reaction, which contributes significantly to the build-up of a proton gradient across the thylakoid membrane. This pH difference is employed by the ATPase to drive the synthesis of ATP from ADP and P_i.

The reactions occurring in PSII can be divided into four processes:

(i) Light harvesting and energy transfer. This is mediated by the chlorophyll and carotenoid molecules of the antenna (A) complexes:

$$Chl_A + h\nu \rightarrow Chl_A^*. \quad (3a)$$

The inner PSII antenna is formed by CP43 and CP47 (Fig. 2A). The captured light energy is then transferred to the reaction center (see below) by exciton transfer according to:[38]

$$Chl_A^* \, Chl_A \rightarrow Chl_A \, Chl_A^*. \quad (3b)$$

(ii) Primary charge separation and stabilization. This occurs in the reaction center (RC), which is an arrangement of four Chl *a* and two Pheo *a* molecules (Fig. 2B) that are bound by the so-called D1 and D2 proteins (Fig. 2A). The overall process can be described by the following sequence:[39]

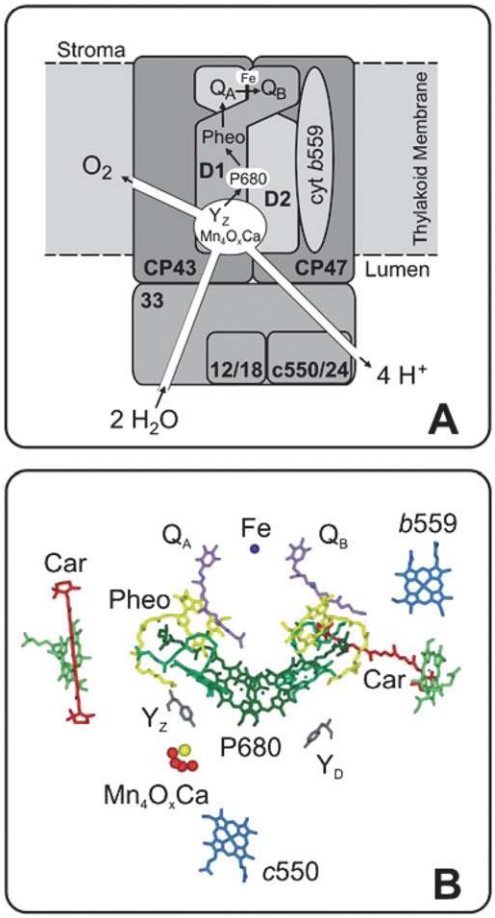

Fig. 2 Simplified scheme of the core components of the water-splitting photosystem II complex that is embedded into the thylakoid membrane of chloroplasts or cyanobacteria (A); adapted from Hillier.[28] Only the relative positioning of the five most important transmembrane subunits and of three extrinsic proteins are shown (the full complex consists of about 20 subunits). The two central subunits are the D1 and D2 proteins. They bind all the electron transfer components. A detailed view of the electron transfer cofactors is given in panel B on the basis of the 3.0 Å crystal structure.[18] In cyanobacteria, cytochrome c550 is part of one of the extrinsic proteins, but has no known function in water-splitting.

$$Chl_A^* \; Chl_{RC} \; Pheo \rightarrow Chl_A \; Chl_{RC}^* \; Pheo \rightarrow Chl_A \; Chl_{RC}^{\bullet +} \; Pheo^{\bullet -}. \quad (4)$$

The radical cation $Chl_{RC}^{\bullet +}$, also known by the absorption maximum of Chl_{RC} as $P680^{\bullet +}$, has an estimated oxidizing potential of +1.2 to 1.3 V, the highest known in biology.[40] PSII therefore requires protection, for example against oxidation or long lived triplet states, ^3Chl, that can form by charge recombination reactions. The two carotenoid molecules, Car, (Fig. 2B) and the cyt *b*559 (Fig. 2A and B) are believed to be involved in this defense system. The primary charge separation is stabilized by electron transfer from $Pheo^{\bullet -}$ to the bound plastoquinone (PQ) molecule Q_A, and by the reduction of $P680^{\bullet +}$ by a redox active tyrosine side chain of the D1 protein, Y_Z. These electron transfer reactions increase the distance between the charged species and decrease the energy difference ΔG. Both factors (together with the subsequent reactions described below) significantly minimize competing recombination reactions, leading to an excellent quantum efficiency of PSII for water-splitting (over 90%),[41,42] but to a less favorable energy efficiency.[43,44]

(iii) Reduction of plastoquinone Q_B by $Q_A^{\bullet -}$ and protonation at the 'acceptor side' of PSII. Q_A is a firmly bound PQ molecule that under normal circumstances can be reduced only to the semiquinone level. In contrast, Q_B is a mobile PQ molecule that leaves after double reduction and protonation (from stroma) its binding pocket and transfers the two electrons to the cytochrome b_6f complex under the release of its two protons into the lumen. Then a fresh PQ molecule binds at the Q_B-site from the pool in the thylakoid membrane:

$$Q_A^{\bullet -} \; Q_B \rightarrow Q_A \; Q_B^{\bullet -} \quad (5a)$$

$$Q_A^{\bullet -} \; Q_B^{\bullet -} + 2H^+_{\;stroma} \rightarrow Q_A \; Q_BH_2 \quad (5b)$$

$$Q_A \; Q_BH_2 + PQ \rightarrow Q_A \; Q_B + PQH_2 \quad (5c)$$

$$PQH_2 + cytb_6f^{ox} \rightarrow PQ + cytb_6f^{red} + 2H^+_{lumen} \quad (5d)$$

The reactions (5a)–(5c) constitute the two-electron gate of the acceptor side of PSII. They further stabilize the charge separation by ensuring that the electrons are transported away from PSII *via* the photosynthetic electron transport chain that finally leads to the reduction of CO_2 to carbohydrates. Reactions (5) also couple the electron transport with a proton translocation that is required for ATP synthesis (see above). The non-heme iron between Q_A and Q_B (Fig. 2) appears to serve mostly a structural role, but it also binds a hydrogencarbonate ion that maybe involved in the protonation of Q_B^{2-}.

(iv) Accumulation of oxidizing equivalents and water-splitting. The tyrosine Z radical, $Y_Z^{\bullet}$, formed by $P680^{\bullet +}$, oxidizes the Mn_4O_xCa cluster. Both components are part of the water-oxidizing complex, WOC (or oxygen evolving complex, OEC; white oval in Fig. 2A) that also includes the functional protein matrix, which not only provides the ligands for metal binding, but is also crucial for constituting a proton network that allows coupling of electron and proton transport, gives flexibility for structural changes of the Mn_4O_xCa cluster during catalysis and regulates substrate water entry and product (H^+ and O_2) release. Although the WOC is at the luminal side of the thylakoid membrane, it is actually close to the center of PSII. This comes from the large luminal extensions of the inner antenna complexes CP43 and CP47 and is also due to the binding of three extrinsic proteins (Fig. 2A). Based on this position of the WOC substrate and product channels most likely exist. These are schematically depicted in Fig. 2A.[28] First indications for such channels have indeed been found in the recent crystal structures.[45,46] After four sequential oxidations of the Mn_4O_xCa cluster by $Y_Z^{\bullet}$, two water-derived oxygens form molecular oxygen, which is released into the medium (see below).

2.2 Geometric structure of the WOC

Several crystal structures of PSII isolated from the thermophilic cyanobacteria *T. elongatus* or *T. vulcanus* were obtained.[18,35,48]

Currently the best resolution is 3.0 Å.[18] While these structures give invaluable insight into the overall arrangement of most cofactors and the arrangement of the different protein subunits, the 'pictures' obtained for the Mn_4O_xCa cluster are rather fuzzy and vary between structures. The reasons for that are (1) the too low resolution (Mn–Mn distances are of the order of 2.7 Å, see below) and (2) the fast reduction of the Mn_4O_xCa cluster that is accompanied by the loss of its structure due to radiation damage caused by radicals that are created by the required intense X-ray beams.[49] Nevertheless, the crystal structures provide an approximate overall shape of the cluster, and also affirm the binding place of Ca next to Mn as previously suggested by EXAFS spectroscopy.[50–52] A breakthrough was recently achieved by combining crystallography and EXAFS measurements. This approach allowed collecting polarized XANES and EXAFS spectra along the three crystallographic axes of PSII single crystals. In this way the large number of previously proposed models for the cluster could be reduced to four very similar models, that all have the same Mn_4 core and differ only in the relative position of Ca and/or the orientation of the Mn_4 unit.[47] One of these structures is shown in Fig. 3 together with a ligand environment that is taken from the crystal structure. The precise bridging motif between Mn and Ca could not be derived and is therefore not shown. It has to be noted that without adjustments the amino acids around the Mn_4O_xCa cluster are not in optimal positions for ligands. This is most likely a consequence of the radiation damage during the crystallographic measurements. Therefore efforts are under way employing QM/MM and DFT calculations to obtain more realistic overall models of the WOC.[53–56] These calculations also take into account further known components of the WOC that were not yet detected by crystallography or EXAFS. These components are the two substrate water molecules (see below) and chloride, Cl^-. While one recent spectroscopic study suggest that Cl^- may not be a direct ligand of manganese,[57] functional studies indicate that it has to be at least in the vicinity of the Mn_4O_xCa cluster.[36] Hydrogencarbonate (bicarbonate), which is important during the photo-assembly of the Mn_4O_xCa cluster,[58] was recently proven not to be a tightly bound constituent of the functional complex.[59–61]

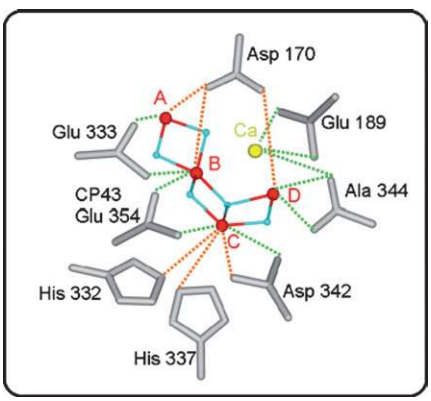

Fig. 3 Structural model (one out of four possible) of the Mn_4O_xCa cluster derived from polarized EXAFS spectroscopy on photosystem II single crystals:[47] Mn (red), oxygen (blue) and Ca (yellow). The model is placed in the EXAFS-derived orientation within the protein ligands determined by crystallography[18] without any optimization. Green lines indicate distances smaller than 3 Å, while orange lines signify distances longer than 3 Å.

Previous EXAFS experiments on frozen PSII-suspensions that were trapped in different S_i states also demonstrate that the Mn_4O_xCa cluster undergoes structural changes during the catalytic cycle[62–64] (see below and Fig. 6). Therefore it is important to note that the structure of the Mn_4O_xCa cluster in the S_1 state (Fig. 3) is, to a yet not fully determined extend, different from that in the S_3 and/or the S_4 states in which the O–O bond is formed.

2.3 Function of the WOC

The Mn_4O_xCa cluster is the 'heart' of the WOC and it fulfils, together with the protein matrix, several vital functions that are outlined in the following.

(i) Coupling of the fast one-electron photochemistry with the slow four-electron water chemistry. The primary charge separation occurs in the reaction center at a time scale of about 3 ps and creates one oxidizing (and one reducing) equivalent at a time.[39] In contrast, for reasons outlined in the next section, water oxidation can only occur once four oxidizing equivalents have been accumulated. This was already shown in 1969 by the period four oscillation of flash-induced oxygen evolution patterns, FIOPs, recorded with dark-adapted PSII samples[66] (for a recent example see Fig. 4A). The different oxidation states through which the Mn_4O_xCa cluster cycles during water oxidation are traditionally referred to as S_i states, where $i = 0, 1, 2, 3, 4$ indicates the number of stored oxidizing equivalents (Kok cycle,[65] Fig. 4B). The S_4 state in this scheme is a postulated, transient state that decays without the need of further light energy into the S_0 state, liberating O_2 and 1–2 H^+. Simultaneously, also one or two substrate water molecules rebind (see below). Time-resolved experiments show that the O_2-release occurs with a half-time of about 1–2 ms.[67,68] Therefore, PSII is able to stabilize, accumulate and synchronize four oxidizing equivalents over a time span of more than nine orders of magnitude to allow the relatively slow water-splitting chemistry to occur.

(ii) Redox-leveling. Every light-induced charge separation in PSII creates the same oxidizing potential of approx. +1.25 V,[40] which reduces to approximately +1.2 V for the $Y_Z^{\bullet}/Y_Z$ redox couple.[69–71] These potentials, although among the highest known for biological systems, are insufficient to allow water oxidation in solution, which requires for the first, most unfavorable step from water to the hydroxyl-radical a potential of more than +2 V. In contrast, concerted water-oxidation in two two-electron steps *via* peroxide, or in a concerted four-electron step is, on average, much less energy expensive and can be realized, if the WOC is constructed in a way that in each of four consecutive steps about the same oxidizing potential is added to the WOC. This requires that the Mn_4O_xCa cluster accumulates oxidizing equivalents, and not charges (one exception is probably the $S_1 \rightarrow S_2$ transition). Consequently, the electron abstractions from the WOC have to be coupled with proton release from PSII, which also results in a decoupling of the release of the two products O_2 and H^+. The established release patterns are: 0 : 0 : 0 : 1 for molecular

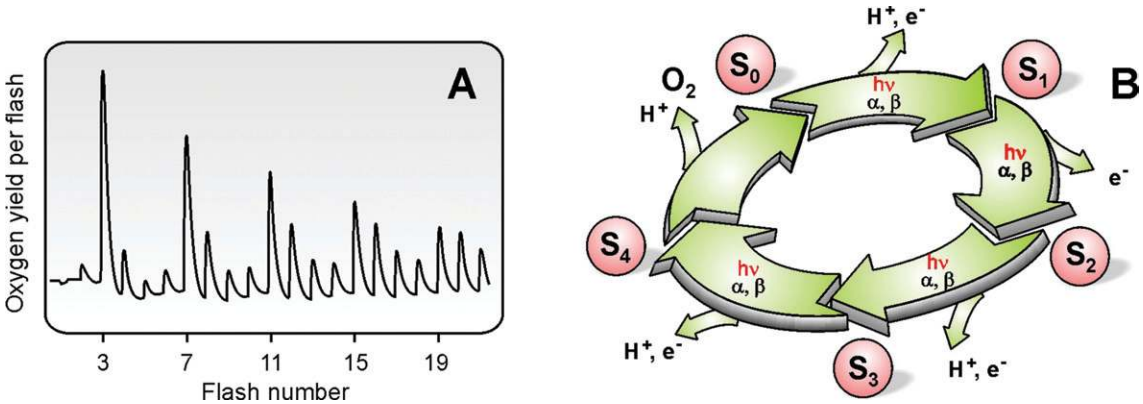

Fig. 4 Flash-induced oxygen evolution pattern (FIOP) of spinach thylakoids measured at 10 °C (Panel A). The period-four oscillation in oxygen-evolution is explained by the Kok-model[65] displayed in Panel B. The different states of the Mn_4O_xCa cluster that are attained after various numbers of light flashes (*hν*) are termed S_i states, where $i = 0, \ldots, 4$ indicates the number of oxidizing equivalents stored in the cluster. The damping of the FIOP is explained by the miss (α) and double hit (β) parameters.

oxygen, and 1 : 0 : 1 : 2 for protons (starting from S_0). For the energy levelling (steps of 0.85, 1.1, 1.15 and 1.0 eV are estimated for the individual S_i state transitions[33]) a coupling of proton and electron transfer is essential, which to a large extent is performed by the specific protein matrix of the WOC that also includes Y_Z. It should be pointed out that in such an optimized system quantum efficiency is more important than energy efficiency for effective water-splitting ($\lambda \leq 680$ nm).

Due to the required high-oxidative power, and the potential formation of harmful side products such as superoxide radicals or peroxides, the lifetime of the WOC and its surrounding D1 protein is limited to less than 30 min in sun light. On the basis of the best known *in vitro* O_2-evolution[72] rates of about 6000 μmol O_2 mg^{-1} Chl h^{-1} (with 35 Chl per reaction center this is equal to a turnover time of 17 ms per released O_2 molecule, which is possibly limited by electron transfer to an artificial acceptor) this corresponds to a total turnover number of about 100 000 O_2 per WOC, while by employing the 1–2 ms O_2 release time an upper estimate of about 1 million turnovers within the life time of a WOC is reached. As will be discussed below most, if not all of the few presently available artificial water-splitting complexes suffer, in a much more severe way, from the same problem. Photosynthetic organisms have devised an efficient repair mechanism to solve this problem. By this mechanism the most damage sensitive part, the D1 protein, is selectively exchanged against a newly synthesized replacement protein. Then the Mn_4O_xCa cluster is reassembled *via* a light-driven process known as photo-activation.[73]

(iii) Substrate water binding and O–O bond formation. An important function of the WOC, and especially of the Mn_4O_xCa cluster, is to bind and activate the water derived oxygens for the O–O bond formation. Thus, localizing their binding sites is of utmost importance for understanding the catalytic cycle of the WOC. To date, neither EXAFS nor X-ray crystallography provide any information on the substrate water binding sites. A possible role of Ca in binding one substrate water has been inferred from time resolved membrane-inlet mass spectrometry (MIMS) studies that employ a rapid jump in $H_2{}^{18}O$ concentration within specific flash sequences,[74,75] and by biochemical Ca/Sr

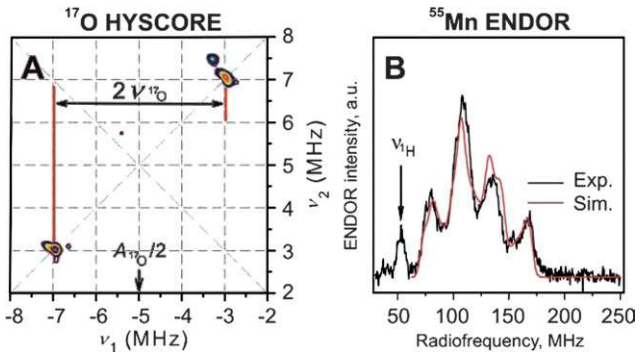

Fig. 5 X-Band ^{17}O HYSCORE (A) and Q-band ^{55}Mn ENDOR (B) spectra of the WOC in the S_2 state spinach PSII membranes. The data were obtained at 4.2 K. For further details see text and refs. 80–82. Reprinted with permission from ref. 80 (A) and 82 (B). Copyright (2007/2008) American Chemical Society.

exchange experiments.[76] The time-resolved MIMS experiments also established that the two substrate molecules bind at separate sites, because their exchange rates vary independently with S_i state.[77] The slower exchanging substrate water can be detected in all S_i states,[74,77] while the exchange of the faster one has only been resolved in the S_2[78] and S_3[79] states. Recently the first clear spectroscopic signature for one bound water was found in the S_2 state by ^{17}O-HYSCORE spectroscopy[80] (Fig. 5A).

Such experiments and their detailed analysis will hopefully allow us in the future to better localize the substrate binding sites. One current suggestion[82] for a binding scenario for the two substrate water molecules in the S_0, S_1 and S_2 states is presented in the bottom row of Fig. 6 (the small black spheres labeled W_s and W_f represent the suggested positions of the oxygens of the slow and fast exchanging substrate water molecules, respectively).

2.4 Electronic structure of the Mn_4O_xCa complex

Detailed information about the electronic structure of the Mn_4O_xCa cluster is key to understanding the mechanism of (water oxidation) in the WOC (see *e.g.* refs. 55 and 82). Since in

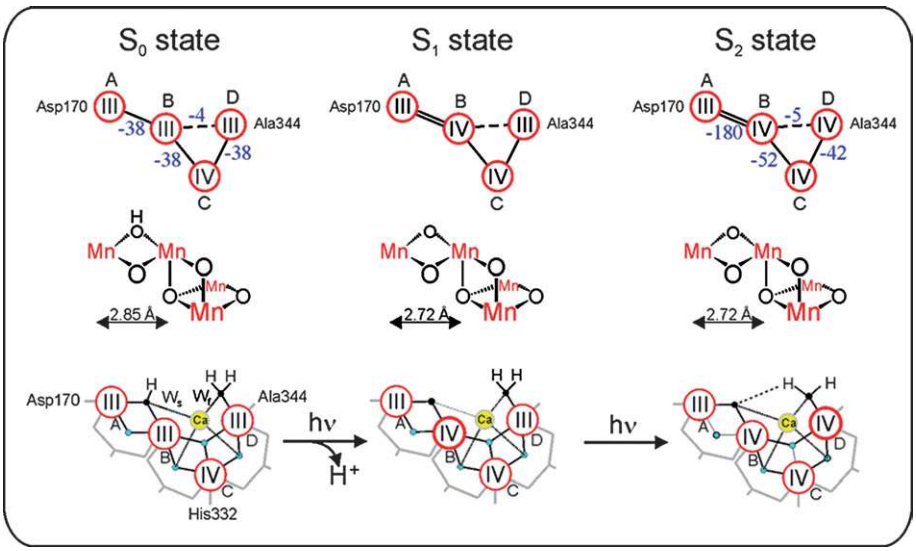

Fig. 6 Schemes of the electronic (top row) and geometric (middle row) structures of the Mn_4 unit within the Mn_4O_xCa cluster as derived from ^{55}Mn-ENDOR[81,82] and EXAFS[47,62,83] spectroscopies in the S_0, S_1 and S_2 states of the water-oxidizing complex of photosystem II. The exchange coupling strength (cm^{-1}) is given in blue numbers and is also symbolized by double lines (strong), single lines (medium strength) and dashed lines (weak) antiferromagnetic coupling. The bottom row shows a possible interpretation of the currently available experimental data on these states, which also includes suggestions for the binding sites of the slowly (W_s) and fast (W_f) exchanging substrate water molecules (small black spheres). Red circles signify Mn ions, bold red circles indicate the Mn ion suggested to be oxidized during the transition. Blue spheres symbolize bridging oxygens. Bridging carboxylate side chains are depicted in grey. Adapted from ref. 82.

each step of the Kok cycle (Fig. 4B) one electron is pulled out of the Mn_4O_xCa cluster (Fig. 3) every second state should be paramagnetic. Indeed cw-EPR signals are known for the S_2[84] and S_0 states.[85–87] In principle these spectra contain all the required information about these two states, but the number of fitting parameters is too large for obtaining conclusive answers. Therefore, recently ^{55}Mn-ENDOR spectroscopy was employed at X-band (S_2 state,[88]) and Q-band (S_2 and S_0;[81,82]) frequencies (Fig. 5(B)). The Q-band studies demonstrated that the S_0 and S_2 states have the overall oxidation states Mn_4(III,III,III,IV) and Mn_4(III,IV,IV,IV), respectively. By also taking information from other spectroscopic measurements into account a tentative assignment of the individual Mn-oxidation states and the exchange coupling constants shown in Fig. 6 (top row) was derived. This also allowed for the first time a specific description of the already known structural change during the $S_0 \rightarrow S_1$ transition[62,64] to a contraction of the Mn_A–Mn_B distance due to the oxidation of one Mn(III) to Mn(IV), which is coupled to a deprotonation of a μ-OH bridge (top two rows in Fig. 6[82]). Together with additional information, for example about the structure and substrate water binding (see above), the tentative reaction scheme for the $S_0 \rightarrow S_1 \rightarrow S_2$ transitions shown in the lower row of Fig. 6 can be suggested.

Other suitable techniques for assessing the Mn oxidation states are XANES (X-ray absorption near edge spectroscopy,[64,89] Kβ-fluorescence spectroscopy[89] and RIXS (resonant inelastic X-ray scattering) spectroscopy.[90] These techniques can probe all S_i states, but the interpretation is also not straightforward, in part due to the lack of suitable theory, in part owing to structural changes between the S_i states that complicate the analysis. While it is now clear that there are Mn(III) to Mn(IV) oxidations during the $S_0 \rightarrow S_1$ and $S_1 \rightarrow S_2$ transitions, it currently remains a matter of controversy whether a similar oxidation happens during the $S_2 \rightarrow S_3$ transition, or whether in this transition a ligand centred oxidation occurs. Similarly the nature of the structural rearrangement between S_2 and S_3 is hotly debated: Dau and co-workers suggest the formation of one additional μ-oxo bridge and thereby the formation of one more short Mn–Mn distance.[64] In contrast, Yachandra and co-workers observe a lengthening of several Mn–Mn distances by 0.1–0.3 Å, which is suggestive of a μ-oxo bridge oxidation within the cluster.[63] Clarification of this controversy will be of utmost importance for understanding the mechanism of photosynthetic water-splitting.

2.5 Suggested mechanisms of O–O bond formation

There is a large number of proposed mechanisms for O–O bond formation in PSII. These have been extensively reviewed in several recent articles.[28,30,33,91] Here only the principles of the currently most favored mechanisms will be briefly summarized.

(A) Nucleophilic attack in the S_4 state. Several different variations of this proposal exist.[26,27,30,55,74,92] The general idea is that a terminal (or bridging; not shown in Fig. 7, top row) oxygen is being prepared for O–O bond formation by turning it during the Kok cycle stepwise into a strong electrophile. In the S_4 state it is fully deprotonated and connected to one (or more) high-valent Mn ions. In the simplest case a terminal Mn(V)=O would be formed, which may also be formulated as Mn(V)≡O^+ or Mn(IV)–$O^{\bullet}$. Alternatively, a μ_2- or μ_3-oxo bridge may act as electrophile (not shown). The electrophile is attacked by a nucleophilic water molecule. This may either be a bulk water molecule, or a water/hydroxo bound to Ca or bridging between Ca and Mn (Fig. 7, top row). Since the water-exchange experiments demonstrate

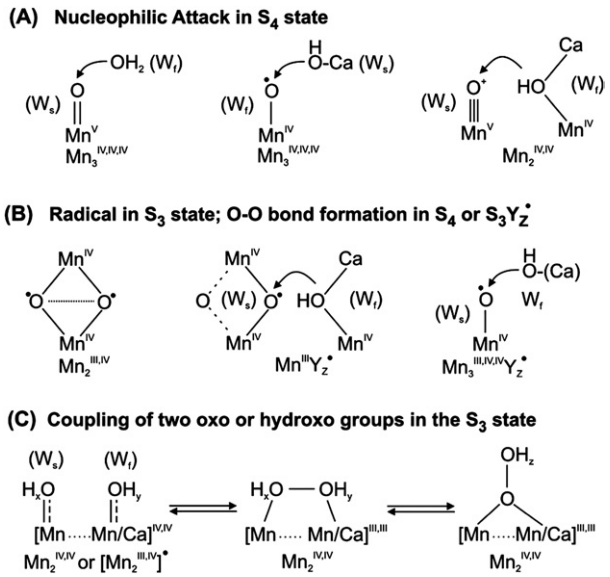

Fig. 7 Suggested routes for O–O bond formation in the water-oxidizing cluster in photosystem II. W_s and W_f indicate the slow and fast exchanging substrate waters, respectively. For further details see the text.

binding of both substrate molecules in the S_3 state, the attack of a free water molecule appears highly unlikely. These type of mechanisms require a Mn(III)→Mn(IV) oxidation during the $S_2 \rightarrow S_3$ transition and another oxidation of the Mn_4O_xCa cluster during the $S_3 \rightarrow S_4$ transition. The latter oxidation is either assumed to be a Mn(IV) → Mn(V) oxidation or a ligand (substrate) based oxidation.

(B) Radical mechanisms. Traditional radical mechanisms assume that already in the S_3 state a ligand centred oxidation occurs.[26,33,63,83,89,93,94] For example, one of the μ-oxo bridges may be oxidized in line with the observed elongation of Mn–Mn distances. Since several Mn–Mn distances change during the $S_2 \rightarrow S_3$ transition also a delocalization of the radical over several bonds (and Mn) may be considered. Since the substrate water exchange rates of the slowly exchanging water are almost identical in the S_2 and S_3 states, this radical would very likely not be identical with W_s. In general two different options are proposed for the further steps leading to O–O bond formation (Fig. 7, middle row): (1) during the $S_3 \rightarrow S_4$ transition a second (bridging) oxygen radical is formed and the O–O bond is created between two radicals in this S_4 state. (2) O–O bond formation is triggered by the $S_3Y_Z^{\bullet}$ state formation, but the Mn_4O_xCa cluster is only oxidized *during or after* the O–O bond formation. In that case a peroxidic intermediate may be formed between the oxygen radical and a water (hydroxo/oxo) molecule bound to Ca and/or Mn. Subsequently, the two-electron reduced cluster with bound peroxide can be easily oxidized by $Y_Z^{\bullet}$, and molecular oxygen is formed and released into the medium under reformation of the S_0 Mn_4(III,III,III,IV)Y_Z state. The critical trigger in the $S_3Y_Z^{\bullet}$ state may be a proton movement initiated during $Y_Z^{\bullet}$ formation (or a hydrogen atom abstraction[95]). Indeed, experimental evidence supporting a rate limiting proton release in this step of the Kok cycle has been put forward.[68,96,97]

(C) O–O bond formation in the S_3 state. In these proposals[32,33,98] it is assumed that the known structural changes during the $S_2 \rightarrow S_3$ transition lead to a situation that in a small fraction of PSII complexes (about 10–15%) a formation of the O–O bond in form of a complexed peroxide occurs already in the S_3 state. This state is assumed to exist within an redox equilibrium of various other forms of S_3 that may include an oxygen radical and/or a Mn_4(IV,IV,IV,IV) state. In addition, different forms of peroxide complexation are possible (end-on *vs.* side-on; Fig. 7, lower row). Once the $S_3Y_Z^{\bullet}$ state is formed, only centers being in the complexed peroxide configuration are assumed to be able of donating an electron to $Y_Z^{\bullet}$ and to liberate O_2. The rate of the $S_3 \rightarrow S_4$ transition would then be limited by the equilibrium constants between the different states, and would follow directly the time course of $Y_Z^{\bullet}$ reduction as observed experimentally. Water exchange would only happen in the majority state in S_3, which would be the open form with two terminal water/hydroxy or oxo groups.

2.6 Summary: Principles of photosynthetic water-splitting

From the above text the following seven principles of photosynthetic water splitting can be extracted:

1. The components of the primary photo-reactions as well as the Mn_4O_xCa cluster are supported by protective components and, once destroyed, automatically replaced by the organism by a specific repair mechanism.

2. A multimeric transition metal complex (Mn_4O_xCa cluster) is employed to couple the very fast one–electron photochemistry with several orders of magnitude slower four electron water-splitting chemistry.

3. The water-splitting catalyst is located in a sequestered environment; channels exist for substrate entry and product release.

4. The matrix (protein) around the Mn_4O_xCa cluster is highly important for the coupling of proton and electron transfer reactions. This feature is essential for achieving about equal redox potentials for all oxidation steps that match the oxidizing potential of the light-generated primary oxidant.

5. Point 4 leads to a decoupling of the release of the two products O_2 and H^+ from the catalytic site.

6. The substrate water molecules are stepwise prepared for O–O bond formation by binding to the Mn_4O_xCa cluster and by (partial) deprotonation. The concerted oxidation of the activated substrate occurs then either in two 2 e^- or one concerted 4 e^- reaction step(s). This avoids high energy intermediates.

7. The Mn_4O_xCa cluster undergoes several structural changes during the Kok cycle, which are probably significant for the mechanism. The surrounding matrix therefore needs to be flexible enough to support such changes.

2.7 Current homogeneous water-splitting catalysts

During billions of years of evolution nature has developed only one light-driven water-splitting catalyst, the above described Mn_4O_xCa cluster. Chemists are not restricted to the abundant, relatively non-toxic Mn, and have therefore created a small number of water-splitting complexes that are based on Ru[99–105] or Ir[106] (for reviews see refs. 13 and 107). These certified

water-splitting catalysts drive water-splitting upon addition of Ce^{IV} or by electrochemistry. Also some Mn-based artificial systems exist,[108,109] but in most cases only a small fraction of the evolved O_2 originates in these latter models from true water oxidation, while the other O_2 molecules contain at least one O-atom from the oxidant, which usually is an oxygen donor such as oxone.[110] One possible exception is a linked di-Mn-porphyrin complex that was demonstrated to evolve correctly labeled dioxygen at defined redox potentials.[111] To the best of our knowledge no visible light-driven homogenous water-splitting catalyst has been reported yet.[112]

The current artificial complexes contain often two metal ions (only one in case of the Ir-complex) that have to undergo several oxidation state changes. In contrast, the four Mn ions in PSII cycle only between oxidation states Mn^{III} and Mn^{IV}. Most complexes are, compared to PSII, still very unstable. Reported total turnover numbers lie between 1 and 3000. Mass spectrometry measurements often reveal in addition to O_2 also CO_2 evolution, which is a result of the oxidation of the organic ligands, either by the added strong oxidants or by the catalysts themselves. Recently a new interesting idea was presented in which two inorganic (SiW_{10}) ligands were employed to stabilize a tetranuclear Ru complex.[113] A stabilizing effect of a clay matrix has also been reported.[114]

While the progress with Ru- or Ir-based catalysts is currently more striking, we regard it still as important to also continue research on Mn-based catalysts, because Ir and Ru are relatively rare, expensive and toxic. Other interesting approaches for achieving light-driven water-splitting employ heterogeneous catalysis on doped TiO_2 (for a review see ref. 115) or $TiSi_2$.[116]

3. Hydrogen conversion

Hydrogen metabolism occurred already very early in evolution. It is established in all domains of life. In fact, it has been proposed that eukaryotic organisms have evolved through a symbiosis of methanogenic archea and hydrogen evolving prokaryots.[117] The enzymes responsible for this metabolism are called "hydrogenases". They catalyze the oxidation of molecular hydrogen into protons and electrons and the reduction of protons to produce molecular hydrogen by a heterolytic mechanism:

$$H_2 \rightleftharpoons H^+ + H^- \rightleftharpoons 2H^+ + 2e^- \quad (6)$$

Hydrogenases are interesting for the development of hydrogen-based fuel cells as well as for "photosynthetic cells" for hydrogen production. Reaction rates for these enzymes are very high; they lie in the range of 10^3–10^4 turnovers per second at 30 °C.[118] It has been shown that hydrogenases when applied to graphite electrodes are as effective as Pt for proton reduction.[119] The catalytic site contains the abundant and inexpensive metals Fe and Ni. A problem is that these enzymes are quite fragile and oxygen sensitive. In the following we will briefly describe structure and function of hydrogenases.

3.1 Hydrogenases

Based on the structure of the active site the enzymes are divided into three classes:

(i) [Fe]-hydrogenases (formerly called metal free hydrogenases) contain one Fe atom coordinated with 2 CO and one H_2O ligand.[120] They are found in methanogenic archea and are exclusively specialized in H_2 oxidation. An organic cofactor (methylenetetrahydromethanopterin) plays an essential role in the catalytic mechanism of this class of enzymes.

(ii) [FeFe]-hydrogenases (formerly called iron-only hydrogenases) contain a unique binuclear Fe cluster which is connected to a conventional cubane [4Fe4S] cluster. Here we find unusual CO and CN^- ligands to the binuclear cluster. These hydrogenases occur in a wide variety of microorganisms, mostly however in anaerobic sulfur reducing bacteria[15,121] and monocellular algae.[122]

(iii) [NiFe] hydrogenases contain a binuclear Ni–Fe complex coordinated by CO and CN^- ligands. This group of hydrogenases is most widely distributed in nature and is relatively well studied.[121,123] The enzymes occur in several types of bacteria living in regions with a higher oxygen concentration.

Quite a few sulfur reducing bacteria contain more than one type of hydrogenase. The family of *Desulfovibrio (D). vulgaris* contains [FeFe] as well as [NiFe] hydrogenases. It is assumed that they are involved in different metabolic functions in different cell compartments.[124,125] The genetic regulation and interplay between these hydrogenases is not yet completely understood.

The increasing interest in renewable energy technology has stimulated the research into hydrogenases, in particular the ones which are active in hydrogen production. Below we review the design principles of the two major classes of hydrogenases ([NiFe] and [FeFe]) and discuss their functional features which may be employed in biotechnological hydrogen production.

3.2 Structural characteristics of hydrogenases

Fig. 8 shows a functional scheme of a hydrogenase enzyme. The substrate/product channels join at the active site where the redox reaction is taking place. The electron flow to and from the active site is relayed over a different path. Most [NiFe] and [FeFe] hydrogenases use "classical cubane" [4Fe4S] clusters for this purpose. Up to now, the crystal structures of five [NiFe]

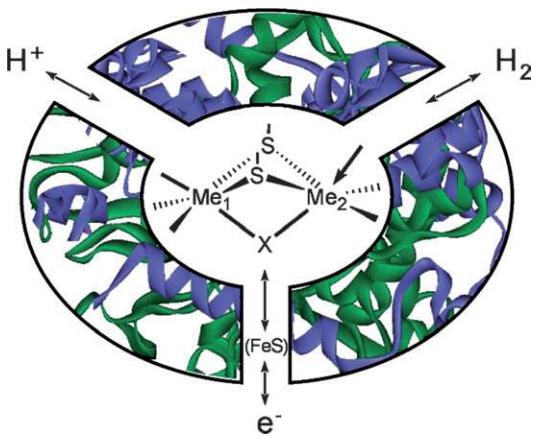

Fig. 8 Schematic representation of a hydrogenase showing the S-bridged bimetallic catalytic center, the H^+ and H_2 channels and the electron transport chain. The open coordination site at one metal is indicated by an arrow.

hydrogenases and two [FeFe] hydrogenases have been determined.[126] They all originate from closely related sulfur reducing bacteria. It is however suspected that the corresponding enzymes from other organisms share the basic structural features of their respective active sites.

3.2.1 [NiFe] hydrogenases. In Fig. 9(A), the structure of the binuclear [NiFe] cluster originating from *D. gigas*[127,128] is shown. The active site is deeply buried inside the large subunit (60 kDa) of the enzyme whereas the smaller 28 kDa subunit harbors two [4Fe4S] clusters and one [3Fe4S] cluster. The distance between the FeS clusters is in the range of 12 Å which is consistent with biological electron transfer.[129] The Ni atom in the active site is bound by four cysteine residues of the protein, two of which form a bridge to the Fe atom which, in turn, is coordinated by two CN^- and one CO ligand. In the most oxidized states of the enzyme (as isolated) an additional bridging ligand X between Fe and Ni is modeled in the crystal structure[130] while in the active reduced states this electron density is absent. Spectroscopic evidence using ^{17}O labeling suggests that this is an oxygen species[131] but the presence of sulfur cannot be ruled out.[130,132,133] The Ni atom has a distorted square pyramidal coordination with a vacant site believed to be the primary binding position of the H_2 substrate. A hydrophobic gas channel has been modeled into the crystal structure using molecular dynamics calculations with a 1 Å probe[134] as well as crystallography under high-pressure Xe gas.[134–136] The channel leads directly from the surface of the protein to the open coordination site of the Ni atom.[134,137] It is assumed that this gas channel is also involved in the reactions with CO and O_2, which inhibit the enzyme. Indeed, comparative crystallography showed that CO and O_2 inhibited [NiFe] hydrogenases show additional diatomic electron density at the open fifth coordination site at Ni.[138] In the oxidized "unready" state of the enzyme, an additional elongated electron density was observed at the bridging ligand "X", suggesting it to be a hydroperoxide OOH^-.[128] It is suggested that the peroxo bridging ligand causes the enzyme to be "locked" in the unready state which can be reactivated only very slowly. In the [NiFe] hydrogenases characterized so far, the catalytic site is located on the large subunit while the electron transport chain is accommodated on the small subunit.

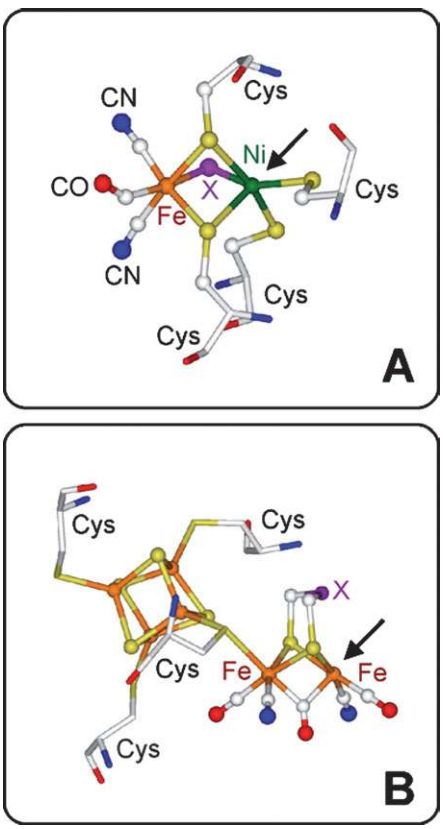

Fig. 9 Catalytic centers of [NiFe] hydrogenase (A) and [FeFe] hydrogenase (B) taken from the respective X-ray crystallographic structures.[127,128,139–141] The putative site of H_2 attachment is indicated by an arrow. For details see the text.

3.2.2. [FeFe] hydrogenases. Fig. 9(B) shows the structure of the H-cluster from the [FeFe] hydrogenase isolated from *Desulfovibrio desulfuricans*.[17,139–141] The active site, a [6Fe6S] cluster is located in the center of the protein. Two additional [4Fe4S] cubane clusters form the electron pathway to the external redox partner of the enzyme. In *C. pasteurianum* three 4Fe4S and one 2Fe2S cluster serve this task while the algal hydrogenases appear to lack the accessory 4Fe4S clusters altogether. In these hydrogenases the H-cluster interacts directly with the ferredoxin redox partner.[142] A hydrophobic gas channel has also been modeled.[140] It ends at the most remote Fe atom (Fe_d) of the active site (see arrow). Finally, a chain of amino acid residues is identified which could act as proton pathway.[140] The H-cluster consists of a classical cubane [4Fe4S] sub-cluster connected to the "catalytic" [2Fe2S] subcluster through a cysteine bridge. The [2Fe2S] sub-cluster has 2 CN^- and 3 CO ligands as well as a peculiar di-thiol ligand bridging the two Fe-atoms. While the [4Fe4S] sub-cluster is connected to the protein matrix in a "classical" way, the [2Fe2S] sub-cluster has no covalent interaction with the protein apart from the cysteine link to the cubane sub-cluster. The dithiol ligand is not unequivocally characterized in the X-ray structures. In particular, the nature of the central atom in the bridge is not yet determined. It can be modeled as a C- or N-atom.[139] Recent modeling studies suggest that the bridging ligand could also be an ether.[143] In particular the occurrence of a nitrogen (or oxygen) would be of mechanistic relevance since the central atom could act as proton acceptor/donor in the hydrogen oxidation/reduction reaction. The crystal structure of the H-cluster is available in three "states" of the protein: In the active oxidized state one of the CO ligands forms a bridge between the two Fe atoms. Upon reduction of the enzyme by H_2, this ligand shifts towards a terminal position on the distal iron atom. Exposure to CO gas is known to inhibit the protein. This is visible in the crystal structure by the appearance of an additional terminal CO ligand in the open coordination site. The CO and CN^- ligands in the crystal structure have been assigned making use of FTIR data as well as taking into account the possibility for hydrogen bonding of the CN^- groups to nearby amino acid residues.[17]

3.3 Active and inactive states of hydrogenases

Similar to the water oxidizing complex in PS II the catalytic site in hydrogenases can exist in several different redox states.

Midpoint potentials have been determined using spectro-electrochemistry.[144–147] Structures of the intermediates resulted from different spectroscopic techniques.[16,148,149] The various states are summarized below.

3.3.1 [NiFe] hydrogenases. In the aerobically 'as isolated' form the [NiFe] hydrogenases are inactive and have to be activated under H_2 or other reductants. The activation process has been studied in great detail using EPR and other spectroscopies.[16,123,147,150,151] The different states and their possible relationships identified in this way are depicted in the scheme presented in Fig. 10. The paramagnetic states are indicated in red. The *as isolated* enzyme is paramagnetic but often shows a mixture of two states, each with a characteristic EPR spectrum, called Ni-A and Ni-B. Ni-A is the "unready" state of the enzyme which takes up to an hour to reactivate. In contrast, Ni-B can be activated within a few minutes. Ni-A is in equilibrium with a singly reduced EPR silent state Ni-SU (silent unready). In oxygen-tolerant species (*e.g. Ralstonia eutropha*) the Ni-A is not observed. It is therefore considered as the oxygen-inhibited state.

Upon reduction of Ni-B the enzyme passes through several EPR silent states: Ni-SIr (silent ready) and Ni-SIa (silent active). These states have been identified using FT-IR spectroscopy.[152,153] After a two-electron reduction the EPR active Ni-C state is reached.[154] In this redox state a hydrogen species has been identified using advanced EPR (HYSCORE, ENDOR) spectroscopy.[155,156] Fig. 11 shows the EPR spectrum of Ni-C as well as its FT-IR spectrum. In addition, the HYSCORE spectrum is depicted obtained from the hydrogenase activated using D_2 in D_2O. The obtained ^2H hyperfine coupling is consistent with a hydride bridging the Ni-Fe unit. Upon illumination of this state at low temperature (<100 K) a different EPR spectrum is obtained assigned to Ni-L.[157,158] It has been shown that the hydride species in Ni-L is dissociated from the Ni-Fe cluster.[155,159] In fact, depending on the temperature and duration

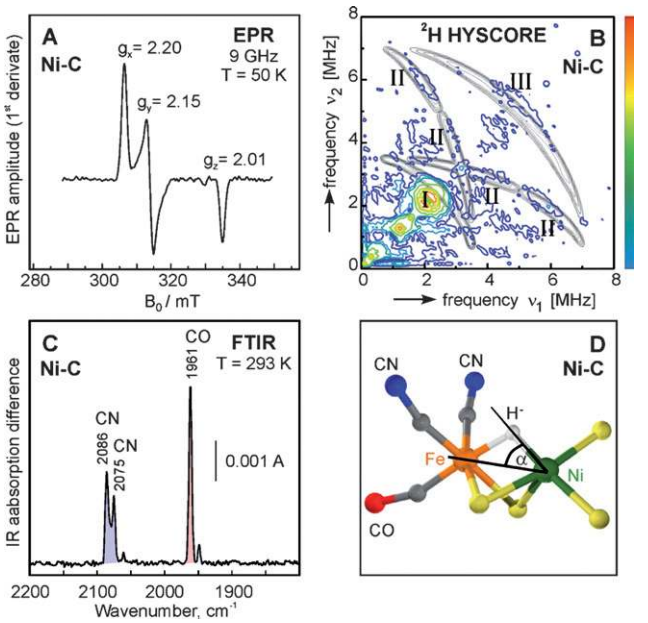

Fig. 11 Spectroscopic characterization of the active Ni-C state of [NiFe] hydrogenase of *D. vulgaris Miyazaki F*: (A) EPR (X-band, frozen state) showing the characteristic *g* tensor components; (B) HYSCORE (X-band at position g_y)[156] showing resonances from a coupled ^{14}N (histidine)[164] and the deuterium in the bridge between Ni and Fe (see panel D). (C) FTIR (room temperature) giving the vibrational frequencies of the CO and two CN^- ligands at the iron, which are characteristic for the Ni-C state. (D) Structural model of the Ni-C state with a bridging hydride, based on the EPR,[165] ENDOR and HYSCORE[156] data. Panel B reprinted with permission from ref. 156. Copyright (2005) Springer-Verlag, Heidelberg.

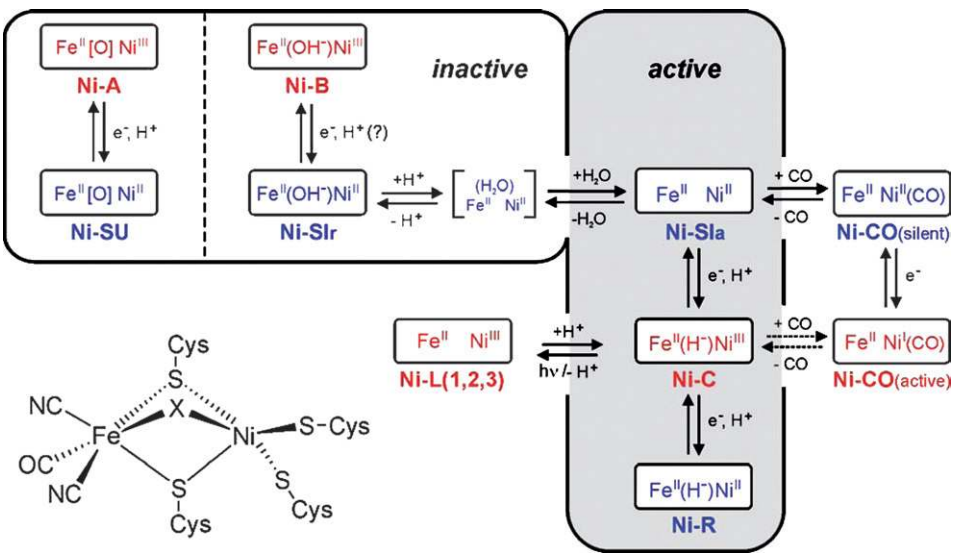

Fig. 10 Scheme representing the different (spectroscopic) states of [NiFe] hydrogenase and their relationship. The formal oxidation states of Ni and Fe are indicated and the bridging ligand X (Fig. 9) is given in parentheses between metals. Paramagnetic (EPR-active) states are red, EPR-silent states blue. The states most probably involved in the catalytic cycle are placed in a shaded box (see also Fig. 13), for details see text and ref. 16. Reprinted with permission from ref 16. Copyright (2007) American Chemical Society.

of the illumination different states Ni-L1, Ni-L2, Ni-L3 can be obtained indicating structural differences of the dissociation products.[160] Raising the temperature above 120 K will recover the original Ni-C state, and the hydride species is shown to be reassociated with the Ni-Fe cluster. A last reduction step from Ni-C produces the EPR-silent Ni-R state which is the most reduced form of the active site. Exposure of Ni-C to CO gas will inhibit the enzyme and a different EPR spectrum Ni-CO(active) is generated.[161] The Ni-CO state is also photosensitive and low-temperature illumination results in the same Ni-L state as obtained from Ni-C. DFT calculations of the electronic structure of the Ni-Fe cluster have been published with possible redox states of the individual Ni and Fe atoms.[162] It is shown that Fe remains Fe(II) throughout all redox reactions. In the most oxidized (inactive) states Ni-A and Ni-B the Ni is proposed to be Ni(III) while in the intermediate reduced states Ni-SU, Ni-SIr, Ni-SIa it is Ni(II). Ni-C on the other hand is believed to have a Ni(III)(H^-)Fe(II) configuration. Finally, the last reduction produces Ni-R in the Ni(II)(H^-)Fe(II) configuration. It is still debated whether the Ni(II) states are low spin (diamagnetic) or high spin ($S = 1$).[163]

3.3.2 [FeFe] hydrogenases. In contrast to most other [FeFe] hydrogenases the enzyme from *D. desulfuricans* can be isolated aerobically. The hydrogenase is however inactive and has to be reductively activated *e.g.* by exposing it to hydrogen gas. This process has been followed spectroscopically using Mossbauer, EPR and FTIR techniques.[149,166–168] In Fig. 12 the different states of the protein which were identified in this way are listed together with the proposed oxidation states of the iron atoms in the binuclear sub-cluster. In the "as-isolated" form, the protein is in an "over-oxidized" state in which both irons are Fe(II). The free

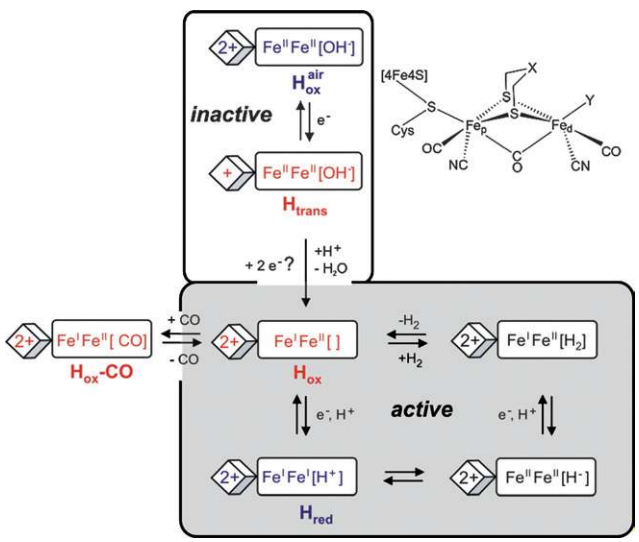

Fig. 12 Scheme representing the different (spectroscopic) states of [FeFe] hydrogenase and their interconversion. The formal oxidation states of the binuclear subcluster and of the distal attached [4Fe4S] cluster are given as well as the putative ligand Y attached to the distal Fe (square brackets). The active states thought to be involved in the catalytic cycle are placed in the shaded box. For further details see text and ref. 16. Reprinted with permission from ref. 16. Copyright (2007) American Chemical Society.

coordination site at the distal iron could be occupied by a water or OH^- ligand. This state of the protein is diamagnetic since also the cubane clusters are oxidized. Activation under hydrogen leads to formation of the active oxidized state (H_{ox}) which has a characteristic rhombic EPR spectrum. It is assumed that the binuclear sub-cluster is in the [Fe_p(I)Fe_d(II)] configuration (see Fig. 12). Continued reductive activation ultimately produces the active reduced state (H_{red}) which is EPR silent but can be identified in FTIR and Mössbauer spectroscopy. It is believed that this state is characterized by a [Fe_p(I)Fe_d(I)] configuration. The enzymatic activity can be effectively inhibited by CO which binds to the open coordination site. The (H_{ox}CO) state has the same electronic configuration as the (H_{ox}) state and shows a characteristic axial EPR spectrum. The inhibiting CO ligand is photolabile and can be photo-dissociated at low temperature (<40 K) with white light leading to formation of the (H_{ox}) state. The EPR spectra of the H_{ox} and H_{ox}-CO state are very characteristic for the H-cluster and are important for understanding the enzymatic mechanism. Among species the differences in *g*-values are relatively small.[169] The spectroscopic investigation of the H-cluster in its various states does not give a clear picture of the actual catalytic mechanism but is does show that the ligand environment of the H-cluster is flexible and that the electrons move to and from the binuclear subcluster *via* the cubane subcluster to the accessory F-clusters. In addition, ^{57}Fe ENDOR and HYSCORE studies[170] have shown that the two subclusters of the H-cluster are in intimate electronic contact.

3.4 Oxygen sensitivity

The oxygen sensitivity of hydrogenases is of great importance with regards to the possible applications in the field of hydrogen fuel production, especially when the enzyme is combined with oxygen producing PSII (mimics). Interesting proposals have been put forward to immobilize PSII and a suitable hydrogenase on electrode surfaces separated by a membrane thus avoiding contact of the hydrogenases with oxygen.[171] At the same time intense activities are deployed to genetically modify hydrogenases (*i.e.* generating mutants) in order to reduce their oxygen sensitivity. A few [NiFe] hydrogenases have been identified which show a surprising oxygen resistance. The membrane bound [NiFe] hydrogenase from *Ralstonia eutropha*[153,172–174] is able to reduce protons (be it at a low rate) under oxygen pressure and recovers within 2 s to full activity when oxygen is removed.[175] The basic structure of the active site in this hydrogenase does not differ from other [NiFe] hydrogenases so the reason for this oxygen resistance is not yet elucidated. In Table 1, a summary is presented on the oxygen sensitivity of various hydrogenases.

The oxygen sensitivity of [FeFe] hydrogenases is even more severe since the H-cluster is irreversibly destroyed upon reaction with oxygen. The Fe centers in the nuclear sub-cluster are probably oxidized to Fe(III) and lose their CO ligands. Nevertheless, some [FeFe] hydrogenase species seem to show a remarkable oxygen tolerance.[176,177] This behavior might be correlated with the properties of the hydrophobic gas channel. It is assumed that H_2 can diffuse much easier through the protein and reach the active site than O_2 and CO. Therefore, much effort is put into the modification of the amino acids in the gas channel in particular of the hydrogenase form *Chlamydomonas*

Table 1 Oxygen sensitivity of various hydrogenases. (pH 6, 30 °C)[a]

Enzyme, in order of position of organism in a pond (top to bottom)	Rate of anaerobic inactivation at pH 6	Rate of activation after anaerobic inactivation	Reaction with O_2	Limiting rate constant for recovery from O_2 ($t_{1/2}$)
Ralstonia eutropha [NiFe]-MBH	Fast	Fast	Fast, reversible	0.34 s^{-1} (2 s)
Allochromatium vinosum [NiFe]-hydrogenase	Slow	Fast	Fast, >90% reversible	4.7×10^{-4} s^{-1} (25 min)
Desulfovibrio gigas [NiFe]-hydrogenase	Slow	Fast	Fast, >70% reversible	3.3×10^{-4} s^{-1} (35 min)
Desulfovibrio desulfuricans [FeFe]-hydrogenase	Fast	Fast	Fast, irreversible	No recovery

[a] Data are taken from Vincent *et al.*[175] Table adapted from ref. 175 with permission. Copyright (2005) American Chemical Society.

reinhardtii.[178–180] But this is certainly not the only effect responsible for the (better) oxygen tolerance of several hydrogenases; also the geometric and electronic structure of the active site might play a role.

3.5. Proposed mechanisms of proton reduction and H_2 oxidation

Hydrogenases, in contrast to PS II, are reversible enzymes and catalyze both hydrogen production and cleavage. In view of technical applications both reactions are interesting for catalysis: H_2 production with regard to solar fuel production, and H_2 cleavage for developing Pt-free fuel cell catalysts.[181]

3.5.1 [NiFe] hydrogenases. Several DFT modeling studies have been performed into the possible mechanisms of hydrogen conversion of the [NiFe] active site.[182–189] It is believed that Ni-SIa, Ni-C and Ni-R are the states which are actually involved in the catalytic cycle. Furthermore, it is assumed that the H_2 binds initially to the Ni atom. This is also the site where the gas channel in the protein ends and nickel binds CO, a competitive inhibitor.[138] Subsequently, the dihydrogen will be heterolytically cleaved leaving a hydride in the active site, most probably as bridging ligand. The proton could be accepted by one of the terminal cysteine ligands. Other studies propose a H_2O loosely bound to the Fe(II) as base.[182] A more recent DFT study suggested that Ni-SIa is not involved in the catalytic cycle and that Ni-C is the starting point of the reaction. Here, a hydride is permanently present in the active site and would act as base for the heterolytic splitting of H_2.[189]

In Fig. 13 the two most recent models of the reaction are depicted. In both versions, H_2 is initially bound to Ni. In the first model the proton is accepted by a loosely bound water to Fe(II), while in the second model it is accepted by the bridged hydride which is permanently present in the active states. In the first model, the Ni center is then reductively protonated (Ni-R) which releases the protons in a two-electron oxidation step. The second model assumes that the two protons are released in two subsequent single electron oxidation steps. Here H_2 splitting is described, but it is assumed that the reverse reaction (H_2 production) will occur through the same (reverse) pathway.

3.5.2 [FeFe] hydrogenases. The possible catalytic mechanisms of [FeFe] hydrogenases are even less well established. This is because (in comparison to [NiFe] hydrogenase) there are less redox states accessible to spectroscopy (*e.g.* EPR), and because the proton accepting base has not been uniquely identified.

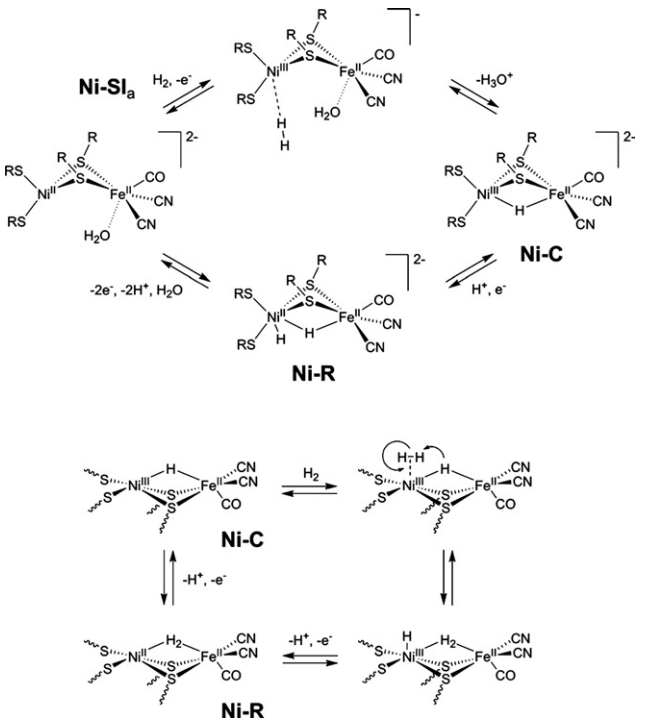

Fig. 13 Two proposed mechanisms for catalytic H_2 oxidation by [NiFe] hydrogenase, see refs. 123, 182 and 189.

Also, the DFT modeling of the reaction cycle is complicated, because the covalently attached cubane [4Fe4S] subcluster probably plays an important role in the electron shuffling, but is very difficult to include in the calculations. In Fig. 14 the most recent model of H_2 production, based on QM/MM calculations is depicted.[190] These calculations include the role of the protein pocket surrounding the H-cluster and assume that the dithiolate bridging ligand contains a center (X) which can act as base accepting protons during the reaction cycle. After reductive activation of the enzyme the OH^- or water ligand at the open coordination site is removed. The binuclear cluster is in the [Fe(II)Fe(I)] oxidation state (H_{ox}). Then, in a further reduction step a proton is transferred to the base X and the binuclear cluster becomes H_{red} [Fe(I)Fe(I)]. The proton is passed to the distal Fe center where it is reduced to a hydride, leaving the binuclear cluster in the [Fe(II)Fe(II)] state. A subsequent reductive protonation will load the base X again and reduce the H-cluster to [Fe(II)Fe(I)]. The proton XH^+ will quickly react with the hydride at the distal Fe and leave as H_2. This will close the reaction cycle producing the active oxidized state again.

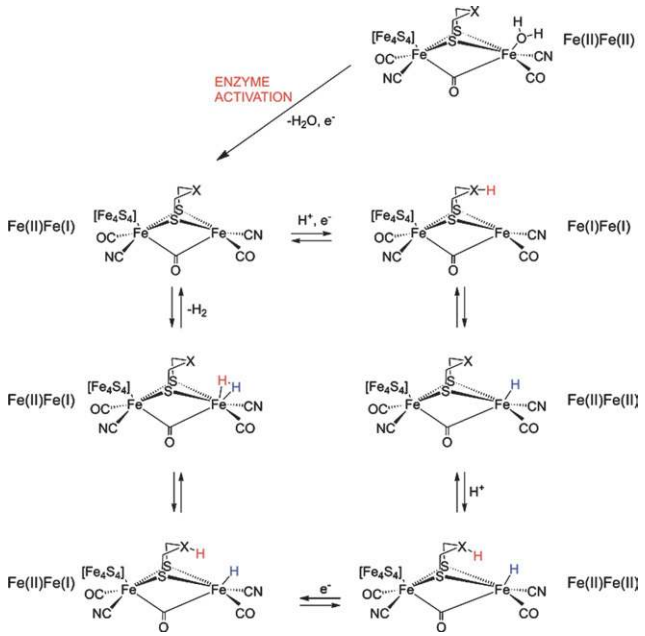

Fig. 14 Proposed mechanism for the catalytic H_2 production by [FeFe] hydrogenase.[190] For details see text. Reprinted with permission from ref. 190. Copyright (2007) American Chemical Society.

3.6 Design principles of hydrogenases

For a better understanding of the design principles of native hydrogenases a comparison of the two major hydrogenases is useful.

The two groups of hydrogenases have a completely different genetic background. Whereas the [NiFe] group is widely distributed in prokaryotes (mostly sulfur reducing bacteria), the [FeFe] group is less widely distributed but occurs in both prokaryots and eukaryots (algae, yeast). In fact, the genetic signature of the H-cluster is found in many higher organisms, even in *homo sapiens*. The [FeFe] hydrogenases are, in general, most active in H_2 production while [NiFe] hydrogenases are more tuned to H_2 oxidation. Both types are however bidirectional. Organisms employing [NiFe] hydrogenases are found in regions with higher oxygen levels than those using [FeFe] hydrogenase. This is because [FeFe] hydrogenases are extremely oxygen sensitive and will be inhibited irreversibly under O_2. [NiFe] hydrogenases are, in general, more oxygen tolerant and some enzymes even evolve H_2 under O_2.

On the other hand, there are many similarities between the basic structures of the active site in both enzymes:

1. Both enzymes employ a bimetallic center where the chemistry is taking place.

2. Both active sites have a "butterfly-shaped" core in which the two metals are bridged by SR-ligands.

3. Only one of these metal atoms is redox active (Ni in [NiFe] and Fe_d in [FeFe] hydrogenase) and they both have a d^7 configuration (Ni(III) and Fe(I), respectively) in their active states.

4. In both catalytic sites the Fe atom is kept at a low valence by the strongly donating ligands CN^- and CO.

5. The metal-metal distance in both structures is short (2.5–2.9 Å), indicating a metal–metal bond.

6. One metal with an open coordination site can be identified in both active states. This is the site where H_2 is believed to bind or is being released.

7. The H/D-isotope effect shows that in both cases the H_2 splitting is heterolytic

8. In both active sites a sulfur or nitrogen/oxygen ligand probably acts as base to accept or donate the H^+.

9. For both enzymes the catalytic activity is often inhibited by O_2 and CO.

These features can serve as guidelines for the construction of biomimetic hydrogenase models.

3.7 Chemical model systems for the active sites in hydrogenases

The reduction of protons to molecular hydrogen – or *vice versa* – seems to be a much easier task to accomplish in model systems than light-induced water oxidation. The extensive structural and functional work on native hydrogenases over the last decade has stimulated the synthesis of a variety of metal-based model systems that might be used as electrocatalysts for hydrogen production or in fuel cells for hydrogen conversion. Considering the high price and low abundance of platinum, which is commonly used for such conversions, there is an urgent need for using sustainable metals such as iron and nickel as employed by nature in the hydrogenases. Important criteria for such catalysts are (i) robustness, *i.e.* a long-term stability, (ii) efficiency (high turnover frequency) and (iii) a low overpotential. These criteria are not easy to meet in model systems.[191]

The work on biomimetic models for [NiFe] and [FeFe] hydrogenase has been described in several recent review articles.[191–200] In this work many of the structural features important for proper function found in the native systems have been successfully incorporated, for example the bimetallic Ni–Fe or Fe–Fe core with rather short metal-metal distances, the sulfur-rich environment (terminal and bridging thiolate ligands), CO/CN ligation of the iron, the incorporation of a base for acceptance of the proton, and more recently of a hydride bridge.[201] However, for none of the structural mimics of the active centers of the native systems a catalytic behavior has been reported so far leading to proton reduction or dihydrogen oxidation.

In this respect, other bioinspired model systems seem to be better suited as discussed in ref. 202. They contain for example dinuclear metal centers with Ru, Re or Ir. For a trinuclear $NiFe_2$ complex[203] some catalytic activity has also been reported. Furthermore, some mononuclear metal complexes catalyze proton electroreduction, but turnover numbers and frequencies are rather low.[191] Recently, a promising dinuclear Ni–Ru complex has been described.[204] It meets most of the criteria for a functional model and directly reacts with and heterolytically splits dihydrogen. This model incorporates a bridging hydride ligand, a crucial factor for proper function in [NiFe] hydrogenase. In the [FeFe] hydrogenase the hydride is most probably bound terminally to the distal iron. It has been proposed to use these differences in hydride binding as a criterion for hydrogenase models instead of the type of metal centers.[202,204]

In summary, *structural* model chemistry of hydrogenases is fairly advanced and nice spectroscopic results have been obtained for several systems, see *e.g.* refs. 201, 205 and 206. However, only a few *functional* models exist to date for

hydrogenases. Their stability and turnover frequencies are still low and for all systems studied so far the overvoltage is very high, which represents a serious problem for their application in biotechnological devices.

An envisaged goal is the photocatalytic hydrogen production and conversion. First results in this promising field have already been described (see *e.g.* refs. 207 and 208 for a related review).

4. Conclusions

In this review the current state of the art in the understanding of the water oxidizing-complex and the hydrogenases is described. During recent years these fields have made considerable progress. However, several details are still missing, *e.g.* in case of water oxidation the exact mechanism of O–O bond formation at the Mn_4O_xCa cluster is not known, and for [FeFe] hydrogenases the crucial step of heterolytic H–H splitting/formation is still under debate.

Understanding these biological processes will guide the progress in different avenues towards solar fuel production. The different attempts in that direction can be grouped as follows:

1. Genetic modification of cyanobacteria to increase their light-induced hydrogen production.

2. Genetic modification to convert existing proteins into artificial water-splitting catalysts that can be expressed, *e.g.* in *E. coli.*

3. *De novo* synthesis of water-splitting metalloproteins.

4. Chemical synthesis of biomimetic/bioinspired homogeneous catalysts, reaction centers and antenna systems.

5. Semiconductor based systems.

6. Heterogeneous catalysts that reduce the over potential during electrolysis and may for example be embedded in functional matrices on the surface of electrodes.

The optimization of biological organisms *via* genetic modifications may be the most promising approach on a short term. This will however require hydrogenases that are insensitive towards oxygen, and are more directly linked to the photosynthetic electron transport chain. Furthermore, competing metabolic reactions (cell growth/biomass production) of these organisms must be reduced by genetic manipulation and/or special culture conditions in order to maximize the H_2 evolution rates so that they approach levels that are relevant for potential applications. Other problems concern the light access (optimization of antenna size), and the required space and costs of the bioreactors.[142,209] Based on studies of the natural systems much has also been learned concerning the design principles required for biomimetic catalysts for water splitting and hydrogen evolution (see above sections). These include the use of abundant and inexpensive metals, the effective protection of the active sites in functional protein environments, and repair/replacement of active components in case of damage. For biomimetic chemistry it is to date clearly in far reach to mimic all these features – but many labs are working towards this goal by developing new approaches in the design and synthesis of such systems, encompassing not only the catalytic center, but also smart matrixes and the assembly *via* self organization.

More stable catalysts that do not require self repair, may be obtained by fully artificial catalytic systems that are totally different from the biological ones and only apply some basic principles learned from Nature. Other metals than Mn/Ca, Fe and Ni could be used, new ligand spheres and other matrices. For light harvesting, charge separation/stabilization and the effective coupling of the oxidizing/reducing equivalents to the redox catalysts different ways have been proposed; *e.g.* covalently linked molecular donor–acceptor systems, photovoltaic devises, semiconductor based systems and photoactive metal complexes (*e.g.* Ru-complexes).[6,210]

The aim of all these approaches is to develop catalytic systems that split water with sun light and produce hydrogen and oxygen, have a high efficiency and a long term stability. If such a system – either biological, biomimetic or bioinspired – has been developed there is hope to use it on a large scale to produce "solar fuels", *e.g.* hydrogen or secondary products thereof. A remaining question is the availability of the sources "light" and "water". The amount of (fresh) water necessary to be split for fuel production, *i.e.* to replace oil and coal on a long term can be estimated on the basis of the total primary energy consumption of Germany to be 30 l per day and person (assuming the same relative power conversion efficiencies for oil and H_2). For 10 h of useable sunlight per day this corresponds to $\approx$ 1 ml H_2O (0.05 mol) per second. For a turnover frequency of 1000 s^{-1} this requires 50 μmol of catalyst per person. Clearly, scientists are currently facing very large challenges to solve these scientific, strategic and logistic problems. But these problems must be overcome – otherwise mankind will not be able to survive when fossil fuels are extinguished on our planet.

Acknowledgements

This work has been supported by the Max Planck Society, the EU/Energy Network project SOLAR-H2 (FP7 contract 212508) and BMBF (Bio-H_2).

References

1 Govindjee, *Advances in Photosynthesis and Respiration*, ed. Govindjee, Springer, Dordrecht, 1994–2008, vol. 1–26.
2 R. E. Blankenship, *Molecular Mechanisms of Photosynthesis*, Blackwell Science Ltd., Oxford, 2002.
3 G. Renger, *Primary Processes of Photosynthesis - Part 1 and 2. Principles and Apparatus*, ed. G. Renger, Comprehensive series in Photochemical & Photobiological Sciences, RSC Publishing, Cambridge, 2008.
4 International Energy Agency (ed.), *World Energy Outlook 2008*, Organisation for Economic Co-operation and Development OECD, 2008.
5 Intergovernmental Panel on Climate Change (ed.), *Fourth Assessment Report*, 2007.
6 N. S. Lewis and D. G. Nocera, *Proc. Natl. Acad. Sci. U. S. A.*, 2006, **103**, 15729.
7 N. Armaroli and V. Balzani, *Angew. Chem., Int. Ed.*, 2007, **46**, 52.
8 R. Cammack, M. Frey, R. Robson, *Hydrogen as a Fuel: Learning from Nature*, Taylor & Francis, London and New York, 2001.
9 P. Hoffmann, *Tomorrow's Energy. Hydrogen, Fuel Cells, and the Prospects for a Cleaner Planet*, The MIT Press, Cambridge, 2002.
10 D. C. J. Sperling, *The Hydrogen Energy Transition: Moving Toward the Post Petroleum Age in Transportation*, Elsevier Academic Press, San Diego, CA, 2004.
11 W. Lubitz and W. Tumas, *Chem. Rev.*, 2007, **107**, 3900.
12 A. F. Collings and Ch. Critchley, *Artificial Photosynthesis: From Basic Biology to Industrial Application*, Wiley-VCH Verlag GmbH, Weinheim, 2005.
13 J. H. Alstrum-Acevedo, M. K. Brennaman and T. J. Meyer, *Inorg. Chem.*, 2005, **44**, 6802.

14 T. J. Wydrzynski and K. Satoh, Photosystem II. The Light-Driven Water: Plastoquinone Oxidoreductase, ed. T. J. Wydrzynski and K. Satoh, in *Advances in Photosynthesis and Respiration*, Springer, Dordrecht, 2005, vol. 22.
15 P. M. Vignais and B. Billoud, *Chem. Rev.*, 2007, **107**, 4206.
16 W. Lubitz, E. Reijerse and M. van Gastel, *Chem. Rev.*, 2007, **107**, 4331.
17 Y. Nicolet, C. Piras, P. Legrand, C. E. Hatchikian and J. C. Fontecilla-Camps, *Struct. Fold. Des.*, 1999, **7**, 13.
18 B. Loll, J. Kern, W. Saenger, A. Zouni and J. Biesiadka, *Nature*, 2005, **438**, 1040.
19 M. Kirch, J. M. Lehn and J. P. Sauvage, *Helv. Chim. Acta*, 1979, **62**, 1345.
20 A. Melis and T. Happe, *Photosynth. Res.*, 2004, **80**, 401.
21 M. L. Ghirardi, P. King, S. Kosourov, M. Forestier, L. Zhang and M. Seibert, Development of Algal Systems for Hydrogen Photoproduction: Addressing the Hydrogenase Oxygen-sensitivity Problem, in *Artificial Photosynthesis*, ed. A. F. Collings and Ch. Critchley, Wiley-VCH Verlag GmbH, Weinheim, 2005, 213.
22 T. Happe, A. Hemschemeier, M. Winkler and A. Kaminski, *Trends Plant Sci.*, 2002, **7**, 246.
23 J. Miyake, Y. Igarashi and M. Rögner, *Biohydrogen III*, Elsevier, Amsterdam, 2004.
24 G. C. Dismukes and R. E. Blankenship, The Origin and Evolution of Photosynthetic Oxygen Production, in *Photosystem II. The Light-Driven Water: Plastoquinone Oxidoreductase*, ed. T. Wydrzynski and K. Satoh, *Advances in Photosynthesis and Respiration*, Springer, Dordrecht, 2005, vol. 22, 683.
25 J. Raymond and R. E. Blankenship, *Coord. Chem. Rev.*, 2008, **252**, 377.
26 J. Messinger, *Phys. Chem. Chem. Phys.*, 2004, **6**, 4764.
27 R. D. Britt, K. A. Campbell, J. M. Peloquin, M. L. Gilchrist, C. P. Aznar, M. M. Dicus, J. Robblee and J. Messinger, *Biochim. Biophys. Acta*, 2004, **1655**, 158.
28 W. Hillier and J. Messinger, Mechanism of Photosynthetic Oxygen Production, in *Photosystem II. The Light-Driven Water: Plastoquinone Oxidoreductase*, ed. T. Wydrzynski and K. Satoh, *Advances in Photosynthesis and Respiration*, Springer, Dordrecht, 2005, vol. 22, 567.
29 N. Nelson and C. F. Yocum, *Annu. Rev. Plant Biol.*, 2006, **57**, 521.
30 J. P. McEvoy and G. W. Brudvig, *Chem. Rev.*, 2006, **106**, 4455.
31 J. Kern and G. Renger, *Photosynth. Res.*, 2007, **94**, 183.
32 G. Renger, *Photosynth. Res.*, 2007, **92**, 407.
33 J. Messinger and G. Renger, Photosynthetic Water Splitting, in *Primary Processes of Photosynthesis - Part 2: Basic Principles and Apparatus*, ed. G. Renger, Comprehensive Series in Photochemical and Photobiological Sciences, The Royal Society of Chemistry, Cambridge, UK, 2008, 291.
34 J. Yano and V. K. Yachandra, *Inorg. Chem.*, 2008, **47**, 1711.
35 K. N. Ferreira, T. M. Iverson, K. Maghlaoui, J. Barber and S. Iwata, *Science*, 2004, **303**, 1831.
36 C. F. Yocum, *Coord. Chem. Rev.*, 2008, **252**, 296.
37 H. J. van Gorkom and C. F. Yocum, The calcium and chloride cofactors, in *Photosystem II. The Light-Driven Water: Plastoquinone Oxidoreductase*, ed. T. Wydrzynski and K. Satoh, *Advances in Photosynthesis and Respiration*, Springer, Dordrecht, 2005, vol. 22, 307.
38 L. M. C. Barter, D. R. Klug and R. van Grondelle, Energy Trapping and Equilibration: A Balance of Regulation and Efficiency, in *Photosystem II. The Light-Driven Water: Plastoquinone Oxidoreductase*, ed. T. Wydrzynski and K. Satoh, *Advances in Photosynthesis and Respiration*, Springer, Dordrecht, 2005, vol. 22, 491.
39 G. Renger and A. R. Holzwarth, Primary electron transfer, in *Photosystem II. The Light-Driven Water: Plastoquinone Oxidoreductase*, ed. T. Wydrzynski and K. Satoh, *Advances in Photosynthesis and Respiration*, Springer, Dordrecht, 2005, vol. 22, 139.
40 F. Rappaport, M. Guergova-Kuras, P. J. Nixon, B. A. Diner and J. Lavergne, *Biochemistry*, 2002, **41**, 8518.
41 J. Messinger and G. Renger, *Biochemistry*, 1994, **33**, 10896.
42 J. Messinger, W. P. Schröder and G. Renger, *Biochemistry*, 1993, **32**, 7658.
43 M. Grabolle and H. Dau, *Physiol Plantarum*, 2007, **131**, 50.
44 L. N. Bell, N. D. Gudkov, Thermodynamics of Light Energy Conversion, in *Topics in Photosynthesis: The Photosystems: Structure, Function and Molecular Biology*, ed. J. Barber, Kluwer Academic Publisher, Dordrecht, 1992, vol. 17.
45 F. M. Ho and S. Styring, *Biochim. Biophys. Acta*, 2008, **1777**, 140.
46 J. W. Murray and J. Barber, *J. Struct. Biol.*, 2007, **159**, 228.
47 J. Yano, J. Kern, K. Sauer, M. J. Latimer, Y. Pushkar, J. Biesiadka, B. Loll, W. Saenger, J. Messinger, A. Zouni and V. K. Yachandra, *Science*, 2006, **314**, 821.
48 N. Kamiya and J. R. Shen, *Proc. Natl. Acad. Sci. U. S. A.*, 2003, **100**, 98.
49 J. Yano, J. Kern, K. D. Irrgang, M. J. Latimer, U. Bergmann, P. Glatzel, Y. Pushkar, J. Biesiadka, B. Loll, K. Sauer, J. Messinger, A. Zouni and V. K. Yachandra, *Proc. Natl. Acad. Sci. U. S. A.*, 2005, **102**, 12047.
50 R. M. Cinco, J. H. Robblee, A. Rompel, C. Fernandez, V. K. Yachandra, K. Sauer and M. P. Klein, *J. Phys. Chem. B*, 1998, **102**, 8248.
51 R. M. Cinco, K. L. M. Holman, J. H. Robblee, J. Yano, S. A. Pizarro, E. Bellacchio, K. Sauer and V. K. Yachandra, *Biochemistry*, 2002, **41**, 12928.
52 R. M. Cinco, J. H. Robblee, J. Messinger, C. Fernandez, K. L. M. Holman, K. Sauer and V. K. Yachandra, *Biochemistry*, 2004, **43**, 13271.
53 E. M. Sproviero, J. A. Gascon, J. P. McEvoy, G. W. Brudvig and V. S. Batista, *J. Am. Chem. Soc.*, 2008, **130**, 3428.
54 S. Zein, L. V. Kulik, J. Yano, J. Kern, Y. Pushkar, A. Zouni, V. K. Yachandra, W. Lubitz, F. Neese and J. Messinger, *Philos. Trans. R. Soc. London, Ser. B: Biol. Sci.*, 2008, **363**, 1167.
55 P. E. M. Siegbahn, *Chem.-Eur. J.*, 2006, **12**, 9217.
56 J. Barber and J. W. Murray, *Coord. Chem. Rev.*, 2008, **252**, 233.
57 M. Haumann, M. Barra, P. Loja, S. Loscher, R. Krivanek, A. Grundmeier, L. E. Andreasson and H. Dau, *Biochemistry*, 2006, **45**, 13101.
58 V. V. Klimov, R. J. Hulsebosch, S. I. Allakhverdiev, H. Wincencjusz, H. J. van Gorkom and A. J. Hoff, *Biochemistry*, 1997, **36**, 16277.
59 C. Aoyama, H. Suzuki, M. Sugiura and T. Noguchi, *Biochemistry*, 2008, **47**, 2760.
60 G. Ulas, G. Olack and G. W. Brudvig, *Biochemistry*, 2008, **47**, 3073.
61 D. Shevela, J. H. Su, V. Klimov and J. Messinger, *Biochim. Biophys. Acta: Bioenergetics*, 2008, **1777**, 532.
62 J. H. Robblee, J. Messinger, R. M. Cinco, K. L. McFarlane, C. Fernandez, S. A. Pizarro, K. Sauer and V. K. Yachandra, *J. Am. Chem. Soc.*, 2002, **124**, 7459.
63 W. C. Liang, T. A. Roelofs, R. M. Cinco, A. Rompel, M. J. Latimer, W. O. Yu, K. Sauer, M. P. Klein and V. K. Yachandra, *J. Am. Chem. Soc.*, 2000, **122**, 3399.
64 M. Haumann, C. Müller, P. Liebisch, L. Iuzzolino, J. Dittmer, M. Grabolle, T. Neisius, W. Meyer-Klaucke and H. Dau, *Biochemistry*, 2005, **44**, 1894.
65 B. Kok, B. Forbush and M. McGloin, *Photochem. Photobiol.*, 1970, **11**, 457.
66 P. Joliot, G. Barbieri and R. Chabaud, *Photochem. Photobiol.*, 1969, **10**, 309.
67 P. A. Jursinic and R. J. Dennenberg, *Biochim. Biophys. Acta*, 1990, **1020**, 195.
68 M. R. Razeghifard and R. J. Pace, *Biochemistry*, 1999, **38**, 1252.
69 J. G. Metz, P. J. Nixon, M. Rogner, G. W. Brudvig and B. A. Diner, *Biochemistry*, 1989, **28**, 6960.
70 K. Brettel, E. Schlodder and H. T. Witt, *Biochim. Biophys. Acta*, 1984, **766**, 403.
71 H.-J. Eckert and G. Renger, *FEBS Lett.*, 1988, **236**, 425.
72 N. Ishida, M. Sugiura, F. Rappaport, T.-L. Lai, A. W. Rutherford and A. Boussac, *J. Biol. Chem.*, 2008, **283**, 13330.
73 S. V. Baranov, G. M. Ananyev, V. V. Klimov and G. C. Dismukes, *Biochemistry*, 2000, **39**, 6060.
74 J. Messinger, M. Badger and T. Wydrzynski, *Proc. Natl. Acad. Sci. U. S. A.*, 1995, **92**, 3209.
75 G. Hendry and T. Wydrzynski, *Biochemistry*, 2003, **42**, 6209.
76 J. S. Vrettos, D. A. Stone and G. W. Brudvig, *Biochemistry*, 2001, **40**, 7937.
77 W. Hillier and T. Wydrzynski, *Biochemistry*, 2000, **39**, 4399.
78 G. Hendry and T. Wydrzynski, *Biochemistry*, 2002, **41**, 13328.
79 W. Hillier, J. Messinger and T. Wydrzynski, *Biochemistry*, 1998, **37**, 16908.

80 J. H. Su, W. Lubitz and J. Messinger, *J. Am. Chem. Soc.*, 2008, **130**, 786.
81 L. V. Kulik, B. Epel, W. Lubitz and J. Messinger, *J. Am. Chem. Soc.*, 2005, **127**, 2392.
82 L. V. Kulik, B. Epel, W. Lubitz and J. Messinger, *J. Am. Chem. Soc.*, 2007, **129**, 13421.
83 V. K. Yachandra, K. Sauer and M. P. Klein, *Chem. Rev.*, 1996, **96**, 2927.
84 G. C. Dismukes and Y. Siderer, *Proc. Natl. Acad. Sci. U. S. A.*, 1981, **78**, 274.
85 J. Messinger, J. H. A. Nugent and M. C. W. Evans, *Biochemistry*, 1997, **36**, 11055.
86 J. Messinger, J. H. Robblee, W. O. Yu, K. Sauer, V. K. Yachandra and M. P. Klein, *J. Am. Chem. Soc.*, 1997, **119**, 11349.
87 K. A. Ahrling, S. Peterson and S. Styring, *Biochemistry*, 1997, **36**, 13148.
88 J. M. Peloquin, K. A. Campbell, D. W. Randall, M. A. Evanchik, V. L. Pecoraro, W. H. Armstrong and R. D. Britt, *J. Am. Chem. Soc.*, 2000, **122**, 10926.
89 J. Messinger, J. H. Robblee, U. Bergmann, C. Fernandez, P. Glatzel, H. Visser, R. M. Cinco, K. L. McFarlane, E. Bellacchio, S. A. Pizarro, S. P. Cramer, K. Sauer, M. P. Klein and V. K. Yachandra, *J. Am. Chem. Soc.*, 2001, **123**, 7804.
90 P. Glatzel, U. Bergmann, J. Yano, H. Visser, J. H. Robblee, W. W. Gu, F. M. F. de Groot, G. Christou, V. L. Pecoraro, S. P. Cramer and V. K. Yachandra, *J. Am. Chem. Soc.*, 2004, **126**, 9946.
91 F. A. Armstrong, *Philos. Trans. R. Soc. London, Ser. B: Biol. Sci.*, 2008, **363**, 1263.
92 V. L. Pecoraro, M. J. Baldwin, M. T. Caudle, W. Y. Hsieh and N. A. Law, *Pure Appl. Chem.*, 1998, **70**, 925.
93 M. Haumann and W. Junge, *Biochim. Biophys. Acta*, 1999, **1411**, 86.
94 P. E. M. Siegbahn, *Inorg. Chem.*, 2000, **39**, 2923.
95 C. W. Hoganson and G. T. Babcock, *Science*, 1997, **277**, 1953.
96 F. Rappaport, M. Blanchard-Desce and J. Lavergne, *Biochim. Biophys. Acta*, 1994, **1184**, 178.
97 M. Haumann, P. Liebisch, C. Müller, M. Barra, M. Grabolle and H. Dau, *Science*, 2005, **310**, 1019.
98 T. J. Meyer, M. H. V. Huynh and H. H. Thorp, *Angew. Chem., Int. Ed.*, 2007, **46**, 5304.
99 S. W. Gersten, G. J. Samuels and T. J. Meyer, *J. Am. Chem. Soc.*, 1982, **104**, 4029.
100 F. P. Rotzinger, S. Munavalli, P. Comte, J. K. Hurst, M. Gratzel, F. J. Pern and A. J. Frank, *J. Am. Chem. Soc.*, 1987, **109**, 6619.
101 R. Zong and R. P. Thummel, *J. Am. Chem. Soc.*, 2005, 127.
102 T. A. Betley, Y. Surendranath, M. V. Childress, G. E. Alliger, R. Fu, C. C. Cummins and D. G. Nocera, *Philos. Trans. R. Soc. London, Ser. B: Biol. Sci.*, 2008, **363**, 1293.
103 M. Rodriguez, I. Romero, C. Sens and A. Llobet, *J. Mol. Catal. A: Chem.*, 2006, **251**, 215.
104 I. Romero, M. Rodriguez, C. Sens, J. Mola, M. R. Kollipara, L. Francas, E. Mas-Marza, L. Escriche and A. Llobet, *Inorg. Chem.*, 2008, **47**, 1824.
105 C. Sens, I. Romero, M. Rodriguez, A. Llobet, T. Parella and J. Benet-Buchholz, *J. Am. Chem. Soc.*, 2004, **126**, 7798.
106 N. D. McDaniel, F. J. Coughlin, L. L. Tinker and S. Bernhard, *J. Am. Chem. Soc.*, 2008, **130**, 210.
107 F. Liu, J. J. Concepcion, J. W. Jurss, T. Cardolaccia, J. L. Templeton and T. J. Meyer, *Inorg. Chem.*, 2008, **47**, 1727.
108 J. Limburg, J. S. Vrettos, H. Chen, J. C. Paula, R. H. Crabtree and G. W. Brudvig, *J. Am. Chem. Soc.*, 2001, **123**, 423.
109 J. Limburg, J. S. Vrettos, L. M. Liable-Sands, A. L. Rheingold, R. H. Crabtree and G. W. Brudvig, *Science*, 1999, **283**, 524.
110 P. Kurz, G. Berggren, M. F. Anderlund and S. Styring, *Dalton Trans.*, 2007, 4258.
111 Y. Naruta, M. Sasayama and T. Sasaki, *Angew. Chem., Int. Ed. Engl.*, 1994, **33**, 1839.
112 C. Herrero, B. Lassalle-Kaiser, W. Leibl, A. W. Rutherford and A. Aukauloo, *Coord. Chem. Rev.*, 2008, **252**, 456.
113 Y. V. Geletii, P. Kögerler, D. A. Hillesheim, D. G. Musaev and C. L. Hill, *Angew. Chem.*, 2008, **120**, 3960.
114 M. Yagi and K. Narita, *J. Am. Chem. Soc.*, 2004, **126**, 8084.
115 M. Yagi and M. Kaneko, *Chem. Rev.*, 2001, **101**, 21.
116 P. Ritterskamp, A. Kuklya, M. A. Wustkamp, K. Kerpen, C. Weidenthaler and M. Demuth, *Angew. Chem., Int. Ed.*, 2007, **46**, 7770.
117 W. Martin and M. Müller, *Nature*, 1998, **392**, 37.
118 H. R. Pershad, J. L. C. Duff, H. A. Heering, E. C. Duin, S. P. J. Albracht and F. A. Armstrong, *Biochemistry*, 1999, **38**, 8992.
119 C. Leger, A. K. Jones, W. Roseboom, S. P. J. Albracht and F. A. Armstrong, *Biochemistry*, 2002, **41**, 15736.
120 S. Shima and R. K. Thauer, *Chem. Rec.*, 2007, **7**, 37.
121 P. M. Vignais, B. Billoud and J. Meyer, *FEMS Microbiol. Rev.*, 2001, **25**, 455.
122 M. L. Ghirardi, M. C. Posewitz, P. C. Maness, A. Dubini, J. P. Yu and M. Seibert, *Annu. Rev. Plant Biol.*, 2007, **58**, 71.
123 W. Lubitz, M. van Gastel and W. Gärtner, *Met. Ions. Life. Sci.*, 2007, **2**, 279.
124 S. A. Caffrey, H. S. Park, J. K. Voordouw, Z. He, J. Zhou and G. Voordouw, *J. Bacteriol.*, 2007, **189**, 6159.
125 I. A. C. Pereira, C. V. Romao, A. V. Xavier, J. LeGall and M. Teixeira, *J. Biol. Inorg. Chem.*, 1998, **3**, 494.
126 J. C. Fontecilla-Camps, A. Volbeda, C. Cavazza and Y. Nicolet, *Chem. Rev.*, 2007, **107**, 4273.
127 A. Volbeda, E. Garcin, C. Piras, A. L. De Lacey, V. M. Fernandez, E. C. Hatchikian, M. Frey and J. C. Fontecilla-Camps, *J. Am. Chem. Soc.*, 1996, **118**, 12989.
128 A. Volbeda, L. Martin, C. Cavazza, M. Matho, B. W. Faber, W. Roseboom, S. P. J. Albracht, E. Garcin, M. Rousset and J. C. Fontecilla-Camps, *J. Biol. Inorg. Chem.*, 2005, **10**, 239.
129 C. C. Page, C. C. Moser, X. X. Chen and P. L. Dutton, *Nature*, 1999, **402**, 47.
130 Y. Higuchi, T. Yagi and N. Yasuoka, *Structure*, 1997, **5**, 1671.
131 M. Carepo, D. L. Tierney, C. D. Brondino, T. C. Yang, A. Pamplona, J. Telser, I. Moura, J. J. G. Moura and B. M. Hoffman, *J. Am. Chem. Soc.*, 2002, **124**, 281.
132 P. M. Matias, C. M. Soares, L. M. Saraiva, R. Coelho, J. Morais, J. LeGall and M. A. Carrando, *J. Biol. Inorg. Chem.*, 2001, **6**, 63.
133 K. A. Vincent, N. A. Belsey, W. Lubitz and F. A. Armstrong, *J. Am. Chem. Soc.*, 2006, **128**, 7448.
134 Y. Montet, P. Amara, A. Volbeda, X. Vernede, E. C. Hatchikian, M. J. Field, M. Frey and J. C. Fontecilla-Camps, *Nat. Struct. Biol.*, 1997, **4**, 523.
135 M. Frey, J. C. Fontecilla-Camps and A. Volbeda, Nickel-iron hydrogenases, in: *Handbook of Metalloproteins*, ed. A. Messerschmidt, R. Huber, T. Poulos and K. Wieghardt, John Wiley & Sons, Ltd., Chichester, 2001, p. 880.
136 A. Volbeda and J. C. Fontecilla-Camps, *Coord. Chem. Rev.*, 2005, **249**, 1609.
137 A. Volbeda and J. C. Fontecilla-Camps, *Dalton Trans.*, 2003, 4030.
138 H. Ogata, Y. Mizogushi, N. Mizuno, K. Miki, S. Adachi, N. Yasuoka, T. Yagi, O. Yamauchi, S. Hirota and Y. Higuchi, *J. Am. Chem. Soc.*, 2002, **124**, 11628.
139 Y. Nicolet, A. L. De Lacey, X. Vernede, V. M. Fernandez, E. C. Hatchikian and J. C. Fontecilla-Camps, *J. Am. Chem. Soc.*, 2001, **123**, 1596.
140 Y. Nicolet, C. Cavazza and J. C. Fontecilla-Camps, *J. Inorg. Biochem.*, 2002, **91**, 1.
141 Y. Nicolet, B. J. Lemon, J. C. Fontecilla-Camps and J. W. Peters, *Trends Biochem. Sci.*, 2000, **25**, 138.
142 A. Hemschemeier, S. Fouchard, L. Cournac, G. Peltier and T. Happe, *Planta*, 2008, **227**, 397.
143 A. S. Pandey, T. V. Harris, L. J. Giles, J. W. Peters and R. K. Szilagyi, *J. Am. Chem. Soc.*, 2008, **130**, 4533.
144 A. L. De Lacey, E. C. Hatchikian, A. Volbeda, M. Frey, J. C. Fontecilla-Camps and V. M. Fernandez, *J. Am. Chem. Soc.*, 1997, **119**, 7181.
145 C. Fichtner, Ch. Laurich, E. Bothe and W. Lubitz, *Biochemistry*, 2006, **45**, 9706.
146 B. Bleijlevens, F. van Broekhuizen, A. L. De Lacey, W. Roseboom, V. M. Fernandez and S. P. J. Albracht, *J. Biol. Inorg. Chem.*, 2004, **9**, 743.
147 S. Best, *Coord. Chem. Rev.*, 2005, **249**, 1536.
148 A. L. De Lacey, V. M. Fernandez, M. Rousset and R. Cammack, *Chem. Rev.*, 2007, **107**, 4304.
149 W. Roseboom, A. L. De Lacey, V. M. Fernandez, C. Hatchikian and S. P. J. Albracht, *J. Biol. Inorg. Chem.*, 2006, **11**, 102.
150 S. P. J. Albracht, *Biochim. Biophys. Acta*, 1994, **1188**, 167.
151 K. A. Vincent, A. Parkin and F. A. Armstrong, *Chem. Rev.*, 2007, **107**, 4366.

152 J. M. C. C. Coremans, J. W. van der Zwaan and S. P. J. Albracht, *Biochim. Biophys. Acta*, 1992, **1119**, 157.
153 B. Bleijlevens, T. Buhrke, E. Van der Linden, B. Friedrich and S. P. J. Albracht, *J. Biol. Chem.*, 2004, **279**, 46686.
154 J. M. C. C. Coremans, C. J. van Garderen and S. P. J. Albracht, *Biochim. Biophys. Acta*, 1992, **1119**, 148.
155 M. Brecht, M. van Gastel, T. Buhrke, B. Friedrich and W. Lubitz, *J. Am. Chem. Soc.*, 2003, **125**, 13075.
156 S. Foerster, M. van Gastel, M. Brecht and W. Lubitz, *J. Biol. Inorg. Chem.*, 2005, **10**, 51.
157 R. Cammack, D. S. Patil, E. C. Hatchikian and V. M. Fernandez, *Biochim. Biophys. Acta*, 1986, **912**, 98.
158 J. W. van der Zwaan, S. P. J. Albracht, R. D. Fontijn and E. C. Slater, *FEBS Lett.*, 1985, **2**, 271.
159 C. Fichtner, M. van Gastel and W. Lubitz, *Phys. Chem. Chem. Phys.*, 2003, **5**, 5507.
160 M. Medina, R. Williams and R. Cammack, *J. Chem. Soc., Faraday Trans.*, 1994, **90**, 2921.
161 R. P. Happe, W. Roseboom and S. P. J. Albracht, *Eur. J. Biochem.*, 1999, **259**, 602.
162 M. Stein, Doctoral Thesis, Technische Universität Berlin, 2001.
163 H. Wang, D. S. Patil, W. Gu, L. Jacquamet, S. Friedrich, T. Funk and S. P. Cramer, *J. Electron Spectrosc. Relat. Phenom.*, 2001, **114-116**, 855.
164 A. G. Agrawal, M. van Gastel, W. Gärtner and W. Lubitz, *J. Phys. Chem. B*, 2006, **110**, 8142.
165 S. Foerster, M. Stein, M. Brecht, H. Ogata, Y. Higuchi and W. Lubitz, *J. Am. Chem. Soc.*, 2003, **125**, 83.
166 D. S. Patil, J. J. G. Moura, S. H. He, M. Teixeira, B. C. Prickril, D. V. DerVartanian, H. D. Peck, J. LeGall and B. H. Huynh, *J. Biol. Chem.*, 1988, **263**, 18732.
167 A. S. Pereira, P. Tavares, I. Moura, J. J. G. Moura and B. H. Huynh, *J. Am. Chem. Soc.*, 2001, **123**, 2771.
168 A. J. Pierik, W. R. Hagen, J. S. Redeker, R. B. G. Wolbert, M. Boersma, M. F. J. M. Verhagen, H. J. Grande, C. Veeger, P. H. A. Mutsaers, R. H. Sands and W. R. Dunham, *Eur. J. Biochem.*, 1992, **209**, 63.
169 C. Kamp, A. Silakov, M. Winkler, E. Reijerse, W. Lubitz and T. Happe, *Biochim. Biophys. Acta*, 2008, **1777**, 410.
170 A. Silakov, E. J. Reijerse, S. P. J. Albracht, E. C. Hatchikian and W. Lubitz, *J. Am. Chem. Soc.*, 2007, **129**, 11447.
171 B. Esper, A. Badura and M. Rögner, *Trends Plant Sci.*, 2006, **11**, 543.
172 T. Buhrke, O. Lenz, N. Krauss and B. Friedrich, *J. Biol. Chem.*, 2005, **280**, 23791.
173 T. Burgdorf, O. Lenz, T. Buhrke, E. Van der Linden, A. K. Jones, S. P. J. Albracht and B. Friedrich, *J. Mol. Microbiol. Biotechnol.*, 2005, **10**, 181.
174 E. Van der Linden, T. Burgdorf, M. Bernhard, B. Bleijlevens, B. Friedrich and S. P. J. Albracht, *J. Biol. Inorg. Chem.*, 2004, **9**, 616.
175 K. A. Vincent, A. Parkin, O. Lenz, S. P. J. Albracht, J. C. Fontecilla-Camps, R. Cammack, B. Friedrich and F. A. Armstrong, *J. Am. Chem. Soc.*, 2005, **127**, 18179.
176 C. Baffert, M. Demuez, L. Cournac, B. Burlat, B. Guigliarelli, P. Bertrand, L. Girbal and C. Leger, *Angew. Chem., Int. Ed.*, 2008, **47**, 2052.
177 S. C. E. Tosatto, S. Toppo, D. Carbonera, G. M. Giacometti and P. Costantini, *Int. J. Hydrogen Energy*, 2008, **33**, 570.
178 J. Cohen, K. Kim, P. King, M. Seibert and K. Schulten, *Structure*, 2005, **13**, 1321.
179 J. Cohen, K. Kim, M. Posewitz, M. L. Ghirardi, K. Schulten, M. Seibert and P. King, *Biochem. Soc. Trans.*, 2005, **33**, 80.
180 M. L. Ghirardi, P. W. King, M. C. Posewitz, P. C. Maness, A. Fedorov, K. Kim, J. Cohen, K. Schulten and M. Seibert, *Biochem. Soc. Trans.*, 2005, **33**, 70.
181 K. A. Vincent, J. A. Cracknell, O. Lenz, I. Zebger, B. Friedrich and F. A. Armstrong, *Proc. Natl. Acad. Sci. U. S. A.*, 2005, **102**, 16951.
182 M. Stein and W. Lubitz, *J. Inorg. Biochem.*, 2004, **98**, 862.
183 L. De Gioia, P. Fantucci, B. Guigliarelli and P. Bertrand, *Inorg. Chem.*, 1999, **38**, 2658.
184 L. De Gioia, P. Fantucci, B. Guigliarelli and P. Bertrand, *Int. J. Quantum Chem.*, 1999, 187.
185 A. L. De Lacey, V. M. Fernandez and M. Rousset, *Coord. Chem. Rev.*, 2005, **249**, 1596.
186 S. Q. Niu, L. M. Thomson and M. B. Hall, *J. Am. Chem. Soc.*, 1999, **121**, 4000.
187 M. Pavlov, P. E. M. Siegbahn, M. R. A. Blomberg and R. H. Crabtree, *J. Am. Chem. Soc.*, 1998, **120**, 548.
188 M. Pavlov, M. R. A. Blomberg and P. E. M. Siegbahn, *Int. J. Quantum Chem.*, 1999, **73**, 197.
189 A. Volbeda and J. C. Fontecilla-Camps, *Top. Organomet. Chem.*, 2006, **17**, 57.
190 C. Greco, M. Bruschi, L. De Gioia and U. Ryde, *Inorg. Chem.*, 2007, **46**, 5911.
191 S. Canaguier, V. Artero and M. Fontecave, *Dalton Trans.*, 2008, 315.
192 M. Y. Darensbourg, E. J. Lyon and J. J. Smee, *Coord. Chem. Rev.*, 2000, **206**, 533.
193 A. C. Marr, D. J. E. Spencer and M. Schröder, *Coord. Chem. Rev.*, 2001, **219**, 1055.
194 T. B. Rauchfuss, *Inorg. Chem.*, 2004, **43**, 14.
195 E. Bouwman and J. Reedijk, *Coord. Chem. Rev.*, 2005, **249**, 1555.
196 V. Artero and M. Fontecave, *Coord. Chem. Rev.*, 2005, **249**, 1518.
197 L. C. Sun, B. Akermark and S. Ott, *Coord. Chem. Rev.*, 2005, **249**, 1653.
198 J. F. Capon, F. Gloaguen, P. Schollhammer and J. Talarmin, *Coord. Chem. Rev.*, 2005, **249**, 1664.
199 X. M. Liu, S. K. Ibrahim, C. Tard and C. J. Pickett, *Coord. Chem. Rev.*, 2005, **249**, 1641.
200 G. J. Kubas, *Chem. Rev.*, 2007, **107**, 4152.
201 L. Schwartz, G. Eilers, L. Eriksson, A. Gogoll, R. Lomoth and S. Ott, *Chem. Commun.*, 2006, 520.
202 C. Mealli and T. B. Rauchfuss, *Angew. Chem., Int. Ed.*, 2007, **46**, 8942.
203 A. Perra, E. S. Davies, J. R. Hyde, Q. Wang, J. McMaster and M. Schröder, *Chem. Commun.*, 2006, 1103.
204 S. Ogo, R. Kabe, K. Uehara, B. Kure, T. Nishimura, S. C. Menon, R. Harada, S. Fukuzumi, Y. Higuchi, T. Ohhara, T. Tamada and R. Kuroki, *Science*, 2007, **316**, 585.
205 S. Löscher, L. Schwartz, M. Stein, S. Ott and M. Haumann, *Inorg. Chem.*, 2007, **46**, 11094.
206 G. Eilers, L. Schwartz, M. Stein, G. Zampella, L. De Gioia, S. Ott and R. Lomoth, *Chem.-Eur. J.*, 2007, **13**, 7075.
207 S. Ott, M. Kritikos, B. Akermark, L. C. Sun and R. Lomoth, *Angew. Chem., Int. Ed.*, 2004, **43**, 1006.
208 M. J. Esswein and D. G. Nocera, *Chem. Rev.*, 2007, **107**, 4022.
209 J. Rupprecht, B. Hankamer, J. H. Mussgnug, G. Ananyev, C. Dismukes and O. Kruse, *Appl. Microbiol. Biotechnol.*, 2006, **72**, 442.
210 S. Fukuzumi, *Eur. J. Inorg. Chem.*, 2008, 1351.